

ABSTRACT

Obesity-induced Alterations to the Immunoproteasome: A Potential Link to Impaired Proteostasis in Skeletal Muscle

Emma Fletcher, Ph.D.

Mentor: Paul M. Gordon, Ph.D.

Effective maintenance of muscle mass is a highly regulated, complex process dependent on a tight balance between muscle protein synthesis and breakdown. Evidence suggests obesity creates a toxic intramuscular environment, which can damage cellular proteins. Such a disruption to proteostasis likely contributes to obese muscle pathology. Although inflammation and/or oxidative stress are considered central to impaired proteostasis, the underlying mechanisms are unclear. Nevertheless, the immunoproteasome (iProt), known to respond to inflammation and oxidative damage, may play a role.

The overarching aims of the studies depicted in this body of work were two-fold. The investigation discussed in Chapter Four sought to elucidate whether a high-fat, high-sucrose diet alters intramuscular iProt content and catalytic activity in wild-type mice to identify a possible mechanism for impaired muscle proteostasis in obesity. Total proteasome content and activity, as well as estimates of muscle oxidative damage, inflammation, muscle mass and strength were also assessed. However, the procedure to analyze iProt activity was previously validated on mouse spleen extracts, and the

translatability to skeletal muscle was unknown. Consequently, Chapter Three describes a preliminary study to optimize the assay protocol in murine skeletal muscle.

The results from Chapter Four demonstrate oxidatively damaged proteins were increased in the muscle of obese mice. These intramuscular alterations also coincided with reduced iProt and total proteasome activity, and reductions in relative muscle mass and strength. Muscle inflammation was unaffected by obesity. Since the proteasome, particularly the iProt, is a prime mediator in the removal of oxidized proteins, our findings suggest proteasome dysfunction could be a key determining event in the loss of intramuscular proteostasis with obesity. As impaired proteostasis diminishes muscle integrity, the inability to contain oxidative protein damage via the proteasome, provides a plausible explanation for the loss of muscle mass and strength noted in the obese mice. Consequently, the results from the study in Chapter Four not only enhance our understanding of proteasome function in obese muscle pathology, but also suggest the proteasome could be a potential therapeutic target to optimize the maintenance of muscle mass and function in obese individuals.

Obesity-induced Alterations to the Immunoproteasome: A Potential Link to Impaired
Proteostasis in Skeletal Muscle

by

Emma A. Fletcher, B.S., M.A., M.S., M.V.B.

A Dissertation

Approved by the Department of Health, Human Performance and Recreation

Paul M. Gordon, Ph.D., M.P.H., Chairperson

Submitted to the Graduate Faculty of
Baylor University in Partial Fulfillment of the
Requirements for the Degree
of
Doctor of Philosophy

Approved by the Dissertation Committee

Paul M. Gordon, Ph.D., M.P.H., Chairperson

K. Leigh Greathouse, Ph.D., M.P.H.,

Grant B. Morgan, Ph.D

Michael Wiggs, Ph.D

Accepted by the Graduate School
August 2021

J. Larry Lyon, Ph.D., Dean

Copyright © 2021 by Emma Fletcher

All rights reserved

TABLE OF CONTENTS

| | |
|---|------|
| LIST OF FIGURES | vii |
| LIST OF TABLES | viii |
| ACKNOWLEDGMENTS | ix |
| CHAPTER ONE | 1 |
| Introduction | 1 |
| Specific Aims – Chapter Three | 4 |
| Specific Aims – Chapter Four | 6 |
| CHAPTER TWO | 10 |
| Literature Review | 10 |
| The Impact of Lipotoxicity on Obese Muscle | 11 |
| The Regulation of Protein Homeostasis in Skeletal Muscle | 14 |
| Conclusions | 21 |
| CHAPTER THREE | 22 |
| The Fluorometric Determination of Immunoproteasome and Total Proteasome Chymotrypsin-like Activity in Murine Skeletal Muscle: An Assay Optimization Study | 22 |
| Introduction | 22 |
| Methods and Materials | 26 |
| Results | 31 |
| Discussion | 35 |
| Conclusions | 38 |
| CHAPTER FOUR..... | 39 |
| Obesity-induced Alterations to the Immunoproteasome: A Potential Link to Impaired Proteostasis in Skeletal Muscle..... | 39 |
| Introduction | 39 |
| Methods and Materials | 43 |
| Results | 51 |
| Discussion | 60 |
| Conclusions | 66 |

| | |
|--------------------|----|
| CHAPTER FIVE | 68 |
| Conclusions | 68 |
| REFERENCES | 74 |

LIST OF FIGURES

| | |
|--|----|
| Figure 3.1. AMC standard curve..... | 32 |
| Figure 3.2. Intensity of AMC fluorescence liberated from skeletal muscle homogenates of varying protein concentrations. | 33 |
| Figure 3.3. Intensity of AMC fluorescence liberated from skeletal muscle homogenate (3 mg protein) in the absence and presence of varying doses of the iProt inhibitor ONX-0914. | 34 |
| Figure 3.4. Intensity of AMC fluorescence liberated from skeletal muscle homogenate (3 mg protein) in the absence and presence of varying doses of the non-specific proteasome inhibitor MG-132..... | 35 |
| Figure 4.1. Change in body mass with high-fat, high-sucrose feeding..... | 52 |
| Figure 4.2. Change in GA muscle mass with DIO. | 53 |
| Figure 4.3. Change in TA muscle mass with DIO..... | 54 |
| Figure 4.4. Change in blood glucose with high-fat, high-sucrose feeding. | 55 |
| Figure 4.5. The impact of high-fat, high-sucrose feeding on forelimb strength..... | 56 |
| Figure 4.6. Change in GA and TA muscle protein carbonyl content in response to high-fat, high-sucrose feeding. | 57 |
| Figure 4.7. Change in GA and TA muscle iProt-specific chymotrypsin-like activity in response to a high-fat, high-sucrose diet. | 59 |
| Figure 4.8. Comparison of iProt-specific and total proteasome chymotrypsin-like activity in the GA muscle of mice with and without DIO.. | 60 |

LIST OF TABLES

| | |
|--|----|
| Table 4.1. Body mass, epididymal fat mass and muscle mass at study completion..... | 53 |
| Table 4.2. A comparison of GA and TA muscle IFN- γ and TNF- α (ng/mg) protein concentrations between obese and normal-weight mice..... | 57 |
| Table 4.3. A comparison of iProt catalytic subunit protein concentrations in the GA and TA muscle of mice with and without DIO | 58 |

ACKNOWLEDGMENTS

There are many individuals who helped me along my doctoral journey that I wish to thank. Foremost, I want to express my gratitude to my advisor, Dr. Paul Gordon for his guidance, support and patience over the last four years. I will also be forever grateful for his willingness to consider and recruit a somewhat non-traditional applicant to the Ph.D. program.

My sincere thanks also go to the rest of my dissertation committee: Dr. Wiggs, Dr. Morgan, and Dr. Greathouse. Your encouragement, insightful comments, technical assistance and advice was truly appreciated.

Besides my committee members, I would like to thank the rest of the faculty, staff and fellow graduate students in the HHPR Department for your unwavering support over the last few years. As well as to mentors and advisors from prior institutions who encouraged my pursuit of a doctoral degree. Dr's. Visich, Durstine and Betts; thank you for not giving up on me after my brief professional deviation into Veterinary Medicine.

I also gratefully acknowledge the funding received towards my dissertation from the HHPR Department Doctoral Dissertation Grant Award. These funds were instrumental for the completion of my research.

Finally, to my family. Words cannot fully describe how grateful I am for your constant support of me and my many educational pursuits. Your patience and understanding are unparalleled.

CHAPTER ONE

Introduction

Obesity can reduce muscle mass and function (1, 8–18), which may be linked to ineffective protein turnover (8, 10, 12, 15, 19, 20). Although chronic inflammation and oxidative stress disrupt protein homeostasis (proteostasis), the underlying mechanisms which coordinate subsequent pathogenic effects in obese muscle are unclear (8, 12, 19). Nevertheless, emerging evidence suggests proteasomes may play a crucial role (21).

The standard 20S and 26S proteasome systems are major cellular pathways responsible for protein degradation (3, 22–26), and essential to prevent the toxic accumulation of misfolded protein aggregates (19, 24, 27, 28) - a hallmark of impaired proteostasis (20, 27, 28). Through these systems, polyubiquitinated and oxidatively modified proteins are degraded via the 26S or 20S proteasomes, respectively (3, 22–26, 28, 29). However, when cells are exposed to oxidative stress or a pro-inflammatory stimulus, the catalytic subunits of the standard proteasomes (β 1, β 2 and β 5) are replaced by the inducible subunits of the immunoproteasome (iProt); β 1i (low molecular mass polypeptide 2 (LMP2)), β 2i (multicatalytic endopeptidase complex-like 1 (MECL-1)) and β 5i (low molecular mass polypeptide 7 (LMP7)) (22, 23, 29–33).

The classically recognized function of the iProt is antigen presentation, and is thus considered an important regulator of the immune response (21, 22, 30, 33, 34). However, additional non-immune, and standard proteasome-analogous functions, such as the degradation of both oxidized and polyubiquitinated intracellular proteins, were recently

revealed (22, 23, 31, 33, 35, 36). Moreover, within pro-inflammatory and/or pro-oxidant cellular environments, iProt upregulation exceeds the 20S proteasome (22, 29, 31, 37), and the 26S proteasome system is transiently inactivated (23, 28, 31, 36, 38, 39). This evidence suggests the iProt has a vital role in sustaining proteostasis, particularly under conditions of inflammation and oxidative stress (29, 31, 37–39).

The iProt may also have muscle-specific functions (40) as iProt suppression promotes intracellular protein oxidation and prevents muscle differentiation in both murine and human skeletal muscle myoblasts (41). Conversely, skeletal muscle concentrations of the LMP7 subunit are increased in several inflammation/oxidative stress-associated atrophic disorders, such as aging sarcopenia (42, 43), muscular dystrophy (44, 45), denervation (46) and other inflammatory myopathies (47). Although the pathological significance of raised LMP7 cannot be inferred from intramuscular concentrations alone (35, 48), the above data suggest the iProt may aid the maintenance of muscle mass, and may become dysregulated in situations of chronic inflammation and/or oxidative stress.

Whether the iProt is altered within obese muscle is unclear. Nevertheless, a preliminary study conducted in our lab found 12-weeks of high-fat feeding significantly increased both oxidative stress (lipid peroxidation) and protein concentrations of the LMP7 subunit in the gastrocnemius (GA) muscle of wild-type (C57BL/6J) mice (49). In contrast, intramuscular inflammation and the concentration of the MECL-1 iProt subunit were unaffected by diet-induced obesity (DIO). Although the increase in LMP7 content could represent a compensatory mechanism to clear oxidatively damaged proteins and regain cellular homeostasis (22, 23, 31, 32), accumulating evidence suggests oxidized

proteins tend to aggregate in situations of chronic oxidative stress (31, 35). Previous research investigating the impact of cellular aging on the standard 20S proteasome demonstrates that while oxidized protein aggregates retain the ability to bind to the outer (i.e., alpha) subunits of the proteasome, these proteins are often too large to enter the catalytic core (50–52). Consequently, further protein aggregation occurs, which may ultimately result in proteasome sequestration-induced inhibition (27, 50, 51, 53). Although iProt enzymatic activity was not assessed in our prior study (49), the alpha-subunits of the iProt and standard proteasomes are structurally identical (23, 31, 35). Thus, the increase in muscle LMP7 content noted in the obese mice of our prior study could conceivably represent inactive or inhibitor-bound units. Considering LMP7 is also required for the post-translational processing and maturation of the LMP2 and MECL-1 iProt subunits (22, 31, 35), such a protein aggregate-induced reduction in LMP7 activity may also explain why intramuscular concentrations of the MECL-1 subunit were unaltered by DIO despite a rise in LMP7 content (49). If the latter is correct, and iProt activity is impaired in obesity, the subsequent inability to contain oxidatively damaged protein accumulation (i.e., maintain proteostasis) via the iProt could ultimately predispose obese individuals to reductions in muscle mass and/or function. As low muscle mass and strength are important predictors of future functional independence, morbidity and mortality (13, 18, 54–59), there is a need to determine potential regulators of muscle proteostasis and how these factors may or may not be altered in the obese state.

Therefore, the overarching aims of the studies depicted in Chapters Three and Four were two-fold. First, the purpose of the investigation discussed in Chapter Four was to elucidate the impact of an obesogenic diet (high-fat, high-sucrose) on intramuscular

iProt content and activity, and whether any alterations to the iProt were associated with intracellular oxidized protein accumulation and reductions in muscle mass and strength in wild-type mice. However, the analytical procedure to assess iProt activity was previously validated on mouse spleen extracts (60), and the translatability to skeletal muscle was unknown. Consequently, Chapter Three describes a preliminary study to optimize the assay protocol listed by the manufacturer in murine skeletal muscle. These optimization trials were completed prior to the investigation of Chapter Four.

A detailed summary of the specific aims for the studies discussed in Chapters Three and Four are listed below.

Specific Aims – Chapter Three

A primary outcome measure of the investigation described in Chapter Four was the assessment of iProt chymotrypsin-like activity in skeletal muscle homogenate of mice with and without DIO. However, the assay protocol previously validated by the manufacturer to determine such activity, was based on mouse spleen extracts (60). As the spleen contains a comparatively higher iProt content than other non-lymphoid tissues (61), the recommended test conditions may not translate to skeletal muscle (62). Therefore, the purpose of the study described in Chapter Three was to optimize the procedures listed by the manufacturer for skeletal muscle. Two specific aims were assessed.

Aim 1 – To Determine Muscle Protein Concentrations Sufficient to Yield Fluorescence Within the Range of the Standard Curve

The purpose of the initial trial was to use the proprietary assay kit to test a range of muscle protein concentrations (1 mg, 3 mg and 5 mg protein) to determine the minimal protein content that would yield sufficient fluorescence signal intensity (i.e., signal within the mid-range of the standard curve) during the assay. Establishing these concentrations were essential to guide final sample protein concentrations to use in future analyses (including those of Chapter Four).

Aim 2 – To Determine the Concentration of iProt- and Standard Proteasome-Specific Inhibitors Required to Appropriately Lower Proteasome Activity in Skeletal Muscle Homogenate

Dose-response trials using the ONX-0914 (iProt-specific) and MG-132 (total proteasome-specific) proteasome inhibitors were performed to test if manufacturer- and surrounding literature-recommended dosages visibly lowered proteasome catalytic activity (i.e., chymotrypsin-like activity) in skeletal muscle homogenate. Observations from these trials, together with manufacturer recommendations and inferences from the surrounding literature, were used to guide inhibitor doses to use in the analyses of Chapter Four.

Specific Aims – Chapter Four

The study described in Chapter Four utilized an established murine model of DIO, known to elicit metabolic derangements that closely resemble the natural progression pattern of human obesity (63–65), to investigate three specific aims.

Aim 1 – To Determine Whether iProt Content and Activity is Altered in the Muscle of Wild-Type Mice with DIO

Although a prior investigation in our lab noted an increase in both intramuscular lipid peroxidation and LMP7 content following 12-weeks of high-fat feeding (49), the pathologic significance is unknown. Moreover, fat content was the only dietary variable manipulated in our previous study and may not fully reflect the derangements which may occur in response to a combined high-fat, high-sucrose (HFS) diet, more consistent with the typical western diet (66). Therefore, the initial aim of the study in Chapter Four was to assess protein concentrations of the three catalytic sub-units of the iProt; LMP2, LMP7 and MECL-1, in muscle homogenate via enzyme-linked immunosorbent assay (ELISA) kits. Considering fast-twitch muscle is more susceptible to lipid stress and accumulation (67, 68), and to minimize possible muscle fiber type-related bias in our results, type II fiber predominant muscles (white gastrocnemius (GA) and tibialis anterior (TA)) (69, 70) were selected for the purpose of this study. Additionally, as DIO may affect weight-bearing (e.g., GA) and non-weight bearing (e.g., TA) muscle groups differentially (18, 71), TA muscles were included in the analyses for comparative purposes.

As physiological significance of the iProt cannot be inferred from cellular presence alone (33, 35, 48, 72), intramuscular iProt chymotrypsin-like activity was also assessed via iProt-specific fluorometric assay kits. The protocol for these assays was first

optimized for use in skeletal muscle homogenate in the study described in Chapter Three. Enzyme activity was normalized to the total proteasome content (i.e., the α -7 subunit) contained within each tissue sample (61, 62, 73, 74). Muscle homogenate treated with the iProt-specific inhibitor, ONX-0914, served as the negative control. Samples treated with MG-132, a non-specific proteasome inhibitor (75, 76), was also assessed for comparative purposes. Due to sample volumes required, MG-132 analyses were only performed in GA muscle homogenate.

Aim 2 – To Compare the iProt Response with the Extent of Oxidized Protein Accumulation in the Muscle of Wild-Type Mice with DIO

Our previous investigation found lipid peroxidation was significantly raised in the GA muscle of mice fed a high-fat diet (HFD) (49). However, the significance of this finding on intramuscular oxidative protein modification and accumulation, could only be inferred. As oxidized protein aggregation (77, 78) could potentially alter proteasomal activity (42, 77), an additional aim of the study in Chapter Four was to assess the concentration of protein carbonyls, a marker of global protein oxidation (77, 78) within the GA and TA of mice fed a HFS diet. Protein carbonyl concentration was analyzed in GA and TA muscle homogenate using the OxiSelect™ Protein Carbonyl ELISA Kit. Protein carbonyl content between lean and obese mice was subsequently compared to iProt content and activity observed in the GA and TA muscle.

Aim 3 – To Determine the Effect of DIO on Muscle Mass and Strength in Wild-Type Mice

Our prior study found GA muscle mass was significantly lower in mice fed a HFD when expressed relative to total body mass. However, absolute muscle mass was significantly increased compared to lean control animals (49), thus rendering the significance of the former findings unclear. Since a HFS diet is more consistent with the typical western diet (66), the study described in Chapter Four sought to determine the combined impact of a high-fat and high-sucrose diet on GA and TA muscle mass of wild-type mice.

Additionally, obesity-associated reductions in muscle contractile function and relative strength (13, 17, 18) are currently considered stronger predictors of future adverse health outcomes (17, 18, 59, 79, 80) and typically manifest prior to a change in muscle mass (59). Consequently, a final aim of the study in Chapter Four was to confirm the effect of DIO on muscle strength assessed via a forelimb weight lifting test (81, 82).

Secondary Outcomes

Our prior study saw no change in markers of pro-inflammatory macrophages, suggesting a HFD does not trigger inflammation within muscle (49). However, intramuscular cytokines were not analyzed. As interferon-gamma (IFN- γ) and tumor necrosis factor-alpha (TNF- α) are considered the most robust pro-inflammatory activators of the iProt (22, 23, 31), and since local inflammation within obese muscle is conflicting (9, 83), protein concentrations of IFN- γ and TNF- α were assessed in GA and TA homogenate of mice with and without DIO via ELISA. Additionally, given that hyperglycemia is a common sequela of an obesogenic diet, which could also impact

intramuscular inflammation and oxidative stress (66, 84, 85), blood glucose was measured in all mice during the feeding phase of the study via a handheld glucometer.

Hypotheses

The primary hypotheses of the investigation of Chapter Four were; intramuscular concentrations of the iProt subunits, protein carbonyls, IFN- γ and TNF- α would be increased, however; iProt activity, and relative muscle mass and strength would be reduced in mice with DIO.

CHAPTER TWO

Literature Review

Obesity is associated with multiple co-morbidities, and previous research suggests reductions in muscle mass, quality and function are potential sequelae (1, 8–18). Evidence obesity disrupts myocellular homeostasis, proteostasis in particular, is mounting, and likely central to the onset of associated pathophysiological changes, such as type II diabetes (14, 15, 19, 20). Although lipotoxicity-induced inflammation and oxidative stress contribute to impaired proteostasis (8, 10, 12, 14, 15, 19), the way in which these stressors are regulated and coordinate subsequent pathogenic effects in obese muscle is still poorly understood (8, 12, 19). Since an inverse relationship between advancing age and muscle mass already exists (86, 87), any molecular perturbations noted in muscle of young obese individuals could exacerbate the loss of muscle which occurs with age. Moreover, as reductions in muscle mass and strength are important predictors of both future morbidity and mortality (13, 18, 54–58), determining potential drivers of muscle atrophy and dynapenia, and how these factors may or may not be altered in the obese state, is now recognized as a scientific priority (8, 20). The following review will discuss recent evidence for a link between obesity-induced lipotoxicity and impaired muscle protein homeostasis, and propose a theoretical mechanism for compromised proteostasis via alterations in intramuscular immunoproteasome content and activity.

The Impact of Lipotoxicity on Obese Muscle

Obesity is a disease of overconsumption and positive energy balance. As nutrient overload becomes chronic, the capacity of adipose tissue (AT) to store surplus fat becomes overwhelmed (1, 8, 10, 20, 88–91). Consequently, non-esterified free fatty acids (FFAs) overflow from the expanding AT mass, to accumulate in ectopic sites, including skeletal muscle (1, 8, 10, 20, 88–92). As muscle and other non-adipose tissues are less equipped to adequately metabolize or store such lipids, an increasingly lipotoxic environment is created, with potential pathologic consequences to cell viability and function (15, 20, 27). Although the fundamental mechanisms involved in lipotoxicity-induced muscle pathology are complex and incompletely understood, oxidative stress and chronic inflammation appear to play an important role (1, 8, 10, 12, 89–91, 93–96).

The Interdependent Relationship Between Obesity, Oxidative Stress and Inflammation

Oxidative stress refers to an imbalance between tissue oxidants and anti-oxidants, which result in an increased production and release of reactive oxygen species (ROS) (14, 22, 23, 27, 93, 95, 97–99). ROS are by-products generated in various cellular processes such as during mitochondrial oxidative metabolism, immune cell oxidative bursts, as well as from nicotinamide adenine dinucleotide phosphate oxidase (NOX) enzymes widely expressed in numerous cells, including adipocytes and muscle (14, 95, 99–101). During these metabolic processes, molecular oxygen is chemically reduced to form unstable free radicals, which include, but are not limited to, the superoxide anion ($O_2^{\cdot-}$), hydrogen peroxide (H_2O_2), and the hydroxyl radical ($\cdot OH$) (93, 95, 98). Under normal/basal cellular conditions, the production of ROS is a tightly regulated process (14, 27, 95, 98).

Transient increases in ROS to moderate/physiologic concentrations is essential for certain

cell functions, such as antioxidant gene expression and the maintenance of redox balance, cell growth, pathogen defense mechanisms, and endothelial function (14, 93, 95, 98, 102). Conversely, ROS cause oxidative tissue injury when production is sustained and cellular concentrations reach supraphysiological levels (14, 98, 102). Key contributors to enhanced ROS production and oxidative stress in obesity include; chronic macronutrient overload to metabolic pathways, an increase in reactive lipid metabolites and inflammation (8, 90, 93–95, 97, 98, 103).

Briefly, excess macronutrient availability and delivery to the glycolytic and lipolytic metabolic pathways generates large amounts of the electron donors NADH (nicotinamide adenine dinucleotide dehydrogenase) and FADH₂ (1,5-dihydroflavin adenine dinucleotide) in the mitochondrial electron transport chain. Such an increase in NADH and FADH₂ facilitates the donation of electrons to molecular oxygen to form disproportionately high levels of ROS, and thus, local oxidative stress (97). In addition, the intramuscular accumulation of excess FFAs stimulates the de novo synthesis of toxic lipid species such as diacylglycerol and ceramides (1, 27, 96, 99, 100, 103, 104). These lipid intermediaries further perpetuate ROS production and oxidative stress via a protein kinase C (PKC)-dependent activation of NOX (103, 104).

The generation of ROS with obesity is also further amplified by the chronic low-grade inflammation, long-recognized to accompany obesity (1, 88, 91, 93, 94, 99, 105, 106). A critical component of inflammation in the obese state is the infiltration of innate and adaptive immune cells, including pro-inflammatory macrophages, T-cells, mast cells and dendritic cells, into AT. Once in situ, activated immunocytes release large amounts of ROS and pro-inflammatory cytokines, creating local inflammation and oxidative

stress. However, these cytokines can also overflow into the systemic circulation, with potential pathologic consequences on peripheral sites, such as muscle (1, 10, 88, 91, 96, 97, 107). For example, cells co-cultured with cytokines consistent with the pro-inflammatory profile of obesity (i.e., TNF- α , interleukin (IL)-1 β , IL-6 and IFN- γ), were shown to significantly increase superoxide production via NOX activation (90, 93, 101). Evidence also suggests TNF- α , IL-1 β and IL-6 produced in response to AT accumulation promote heightened ROS production from tissue-resident leukocytes (28, 94, 97). Moreover, ROS can activate the nuclear factor- κ B (NF- κ B) and c-Jun N-terminal Kinase (JNK) signaling cascades to further upregulate pro-inflammatory gene expression, resulting in a pro-inflammatory, pro-oxidant paracrine loop (93, 94, 97).

Ultimately, the convergence of the above mentioned stressors creates an increasingly oxidative cellular environment, which can be highly damaging to cells and cellular molecules (27). Due to their relative abundance, both intracellular lipids and proteins are prime targets (27, 37). Indeed, the accumulation of lipids within cells not only promotes ROS production, but lipids are also highly susceptible to ROS modification. Specifically, in situations of oxidative stress, ROS peroxidation of intracellular FFAs generates reactive lipid aldehydes (27), such as 4-hydroxy-2-nonenal (4-HNE), 4-hydroxy-hexenal (4-HHE), malondialdehyde, acrolein, and prostaglandin-like end-products (isoprostanes) (27, 28). Notably, such modifications appear to occur within obese skeletal muscle. For example, a preliminary study conducted in our lab found that 12-weeks of high-fat feeding (45% kcal fat) induced lipid peroxidation (8-isoprostane) ($p = .006$) in the GA muscle of wild-type (C57BL/6J) mice, presumably through enhanced intramuscular oxidative stress (49). Although the pathologic

significance in obese muscle is unconfirmed, lipid aldehydes are known to be highly reactive due to the electron-withdrawing property of their carbonyl and hydroxyl oxygen atoms, and capable of damaging all cellular components, including protein (27, 28). Moreover, protein carbonylation via these reactive lipid aldehydes is a common and irreversible post-translational loss-of-function modification, and their aggregation is considered a hallmark of impaired proteostasis induced by oxidative stress (2, 20, 27, 28, 108, 109).

As proteins are key components of muscle, protein quality control (i.e., maintaining protein homeostasis) is vital for optimal function (19, 110). Considering the aggregation of oxidatively damaged proteins is noted with aging sarcopenia (43, 111), and intramuscular fat infiltration increases with age (112, 113), such a disruption to proteostasis could conceivably be a determining event in the loss of muscle integrity and function thought to occur with obesity, and warrants investigation.

The Regulation of Protein Homeostasis in Skeletal Muscle

The maintenance of intramuscular protein homeostasis is dependent on a tight balance between muscle protein synthesis (MPS) and muscle protein breakdown (MPB) (1–7). However, sustaining proteostasis is inherently challenging given the various external and endogenous stressors that accumulate in obese muscle (1, 2, 8, 12, 90, 93–95). Although there is some evidence to suggest MPS is reduced in obesity, numerous studies show no impediment (4). Consequently, disruption to proteostasis with obesity is more likely a function of altered MPB.

A certain amount of MPB is considered an essential quality control mechanism to selectively rid cells of old, misfolded, and/or damaged proteins. Muscle atrophy can

occur if this process is over- or under-active (1–4). For example, even a slight acceleration in MPB, if sustained, can cause a reduction in muscle mass (2, 3). However, this is equally true if MPB is underactive, as the excess strain of damaged protein accumulation can ultimately trigger cellular dysfunction and death (2). Therefore, given the potential pathologic consequences of altered MPB, cells rely on a network of protein quality control systems to regulate proteostasis (19, 24, 111, 114–116).

Skeletal muscle contains several proteolytic mechanisms; however, the proteasome and autophagy-lysosomal systems are the most active in regard to muscle protein turnover (25, 28, 48, 111, 116). The primary function of the autophagy-lysosomal pathway is the degradation of bulk proteins, such as whole organelles, membrane-bound proteins and large unfolded cytosolic proteins (24, 28, 48, 116). In contrast, the proteasome system is vital for the proteolytic breakdown of damaged, modified (e.g., oxidized), defective and/or partially unfolded proteins (3, 24, 26, 28, 48, 116). Although the coordinated actions of both systems are required to maintain intracellular proteostasis, the proteasome system is considered the key regulator of proteolysis in skeletal muscle (3, 19, 25, 48, 111). Moreover, as cell culture and murine model research suggests intramuscular autophagy is unaffected by obesity (92, 117), the focus of the current review is on the regulation and potential dysregulation of the proteasome system.

Proteasome Regulation of Protein Homeostasis – The Standard Proteasome Pathway

The standard proteasome system is constitutively expressed in all eukaryotic cells and comprised of two structurally similar, but functionally different proteasomes; the 20S and 26S proteasomes. Both proteasome variants are large, multi-subunit complexes involved in protein degradation, and contain the 20S proteasome as their core unit (3, 22–

26). Specifically, the 20S proteasome is a cylindrical protein structure consisting of four stacked rings; two identical outer alpha (α) rings, each containing seven distinct α -subunits, and two identical inner beta (β) rings with seven unique β -subunits (22, 23, 31). The β 1, β 2 and β 5 subunits are the proteolytically active components, and display caspase-like, trypsin-like and chymotrypsin-like enzymatic activity, respectively. In contrast, the α rings facilitate substrate recognition (e.g., damaged proteins) and association, as well as the recruitment of regulator proteins (22, 23, 25, 26, 31). The key function of the 20S proteasome is the removal of oxidatively modified and unfolded proteins, the activity of which is enhanced when the α rings bind to an 11S regulator protein (24, 25, 29, 31). Conversely, the addition of ATP-dependent 19S regulatory complexes to both ends of the 20S core unit produces the 26S proteasome, which preferentially degrades polyubiquitinated proteins (3, 19, 24, 25, 31, 111). Therefore, proteins must first be labeled via the covalent attachment of ubiquitin (an 8 kDa polypeptide) chains to be recognized and destroyed by the 26S proteasome (19, 24, 25, 111). This protein labeling occurs through the sequential action of three different ubiquitin enzymes: the ATP-dependent E1 (ubiquitin activating) enzymes, the E2 (ubiquitin conjugating) enzymes, and the E3 ubiquitin ligases, ultimately responsible for transferring ubiquitin to the protein substrate (19, 111). Although many E3 ligases exist, muscle RING finger 1 (MuRF1) and muscle atrophy F box (MAFbx)/Atrogin-1 are considered the primary ligases regulating ubiquitination in skeletal muscle (25).

Potential Alterations to the Standard Proteasome System with Obesity

Disruption to the 20S and/or the 26S proteasomes impairs proteostasis and is associated with pathological states, including muscle atrophy (19, 25, 111). Several reports suggest obesity-associated systemic inflammation and/or oxidative stress upregulates the 26S proteasome, and thus proteolysis, in the muscle of obese mice and rats (16, 83, 118). However, these conclusions are solely based on observed increases in one or both of the previously mentioned E3 ligases, and not 26S-specific activity. Furthermore, in an investigation where chymotrypsin-like activity was assessed, Turpin et al. (117) found a significant reduction in the vastus muscle of wild-type (C57BL/6J) mice with DIO. Consequently, increased intramuscular protein ubiquitination with obesity does not necessarily imply a commensurate upregulation in 26S activity, and results of studies without these measurements should be interpreted with caution. Moreover, in vitro analyses of 26S activity show the 26S proteasome is extremely susceptible to transient oxidative stress-induced inhibition. Such inactivation occurs via the removal, and temporary sequestration of the 19S regulatory proteins, coordinated by Extracellular Matrix Protein 29 (ECM29) and Heat Shock Protein 70 (HSP70), respectively (29, 31, 77, 119). As oxidative stress is common in obesity (1, 8, 12, 90, 93–95), subsequent 26S inactivation is plausible. Thus, alterations to muscle proteostasis in the obese state may be a result of reduced, rather than increased proteasome function, and characterized by an accumulation of ubiquitin-tagged proteins.

Alternatively, a reduction in the 26S proteasome could be a compensatory mechanism considering the 26S proteasome is extremely poor at degrading oxidatively damaged proteins (29, 31, 37, 109). Therefore, stress-induced 26S disassembly may be an

attempt to free additional 20S proteasomes to contend with an increase in oxidized proteins (31). However, the findings and methodologies of Turpin et al. (117), would suggest otherwise. Although these investigators observed reduced chymotrypsin-like activity in obese animals, the $\beta 5$ subunit responsible for such activity, is not exclusive to the 26S proteasome, but shared by both standard proteasome variants (22, 23, 25, 26, 31). Similarly, the negative control (proteasome inhibitor, MG-132) Turpin et al. (117), selected to assess $\beta 5$ activity is not 26S-specific (48, 76). Therefore, there is reason to believe 20S function is also impaired with obesity, and warrants investigation. Nevertheless, the removal of oxidized proteins can be achieved by one other proteasome variant; the immunoproteasome (iProt).

The Immunoproteasome and Protein Homeostasis

Unlike the two standard proteasomes, the iProt is not constitutively expressed in all cells, but induced in situations of cellular stress. Specifically, in the presence of oxidative stress or a pro-inflammatory stimulus, IFN- γ and TNF- α in particular, the catalytic subunits of the standard 20S proteasome ($\beta 1$, $\beta 2$, $\beta 5$) are replaced by those of the iProt ($\beta 1i$ (LMP2), $\beta 2i$ (MECL-1) and $\beta 5i$ (LMP7)), which have enhanced chymotrypsin-like, but lower caspase-like activity (22, 23, 29, 31, 32, 120). This slightly altered enzymatic profile allows for distinct proteolytic activities that generate peptides with a high affinity for major histocompatibility complex (MHC) class I antigen presentation. Consequently, the traditionally recognized function of the iProt is immunological. However, additional, standard proteasome-analogous functions were recently revealed, such as the degradation of both oxidized and polyubiquitinated intracellular proteins (22, 23, 31, 35). Moreover, head-to-head comparisons show the

iProt is more effective than the 20S proteasome in removing oxidatively damaged proteins (29, 36), and the catalytic subunits of the iProt are also preferentially upregulated over the 20S proteasome in situations of inflammation and/or oxidative stress (22, 23, 29, 31, 37). When compared to the 26S proteasome, the iProt is considered as efficient, if not more efficient in the destruction and elimination of ubiquitinated proteins (36, 38, 39). This evidence suggests the iProt has a vital role in maintaining intracellular protein homeostasis (23, 31, 35), and iProt dysregulation is implicated in the pathogenesis of numerous diseases, including experimental colitis, thyroiditis, arthritis, auto-immune neuritis, diabetic nephropathy, abdominal aortic aneurysms and certain cancers (40, 120–125).

The iProt may also have other important muscle-specific functions (40, 41). For example, Cui et al. (41) report that iProt suppression via short hairpin RNA increased intracellular protein oxidation and prevented muscle differentiation in both murine C2C12 and human skeletal muscle myoblasts. Conversely, skeletal muscle concentrations of the LMP7 subunit are increased in several inflammation-associated atrophic disorders, such as aging sarcopenia (42, 43), muscular dystrophy (44, 45), denervation (46) and other inflammatory myopathies (47). Although the pathological significance of raised LMP7 cannot be inferred from intramuscular concentrations alone (35, 48), the above data suggest the iProt may aid the maintenance of muscle mass, and may become dysregulated in situations of chronic inflammation and/or oxidative stress.

Whether iProt activity is altered within obese muscle is currently unclear. Nevertheless, a preliminary study conducted in our lab found 12-weeks of high-fat feeding significantly increased both oxidative stress (lipid peroxidation) and protein

concentrations of the LMP7 subunit in the GA muscle of wild-type (C57BL/6J) mice (49). In contrast, intramuscular inflammation and the concentration of the MECL-1 iProt subunit were unaltered by high-fat feeding. Although the increase in LMP7 content could represent a compensatory mechanism to clear oxidatively damaged proteins and regain cellular homeostasis (22, 23, 31, 32), accumulating evidence suggests oxidized proteins tend to aggregate in situations of chronic oxidative stress (31, 35). Previous research investigating the impact of cellular aging on the standard 20S proteasome demonstrates that while oxidized protein aggregates are able to bind to the outer α -subunits of the proteasome, these proteins are often too large to enter the catalytic core (50–52). Consequently, further protein aggregation occurs, which may ultimately result in proteasome sequestration-induced inhibition (27, 50, 51, 53). Although iProt enzymatic activity was not assessed in our prior study (49), the α -subunits of the standard- and immunoproteasomes are structurally identical (23, 31, 35). Thus, the increased intramuscular LMP7 content noted in the obese mice of our prior study could conceivably represent inactive or inhibitor-bound units. Given that LMP7 is also required for the post-translational processing and maturation of the LMP2 and MECL-1 iProt subunits, (22, 31, 35), such a protein aggregate-induced reduction in LMP7 activity may also explain why raised intramuscular oxidative stress failed to stimulate an increase in the MECL-1 subunit in the obese mice of our prior study. If the latter is correct, and iProt activity is impaired in obesity, the subsequent inability to contain oxidatively damaged protein accumulation (i.e., maintain proteostasis) via the iProt could ultimately predispose obese individuals to reductions in muscle mass and/or function. As muscle atrophy is an important predictor of future functional independence, morbidity and

mortality (13, 18, 54–58), determining whether altered iProt function contributes to obese muscle pathology requires further confirmation.

Conclusions

Effective maintenance of muscle mass is a highly regulated, complex process dependent on a tight balance between muscle protein synthesis and breakdown (1–7). Research over the last five decades highlight the critical role of the standard proteasome in sustaining protein homeostasis, and how aberrations in this proteolytic system are linked to numerous diseases, including muscle atrophy (19, 25, 111, 126–128). Nevertheless, the growing evidence for the iProt to play a part in intramuscular proteostasis cannot go ignored (41–47, 49).

As numerous exogenous and endogenous stressors are known to accumulate in obese muscle (1, 8, 12, 90, 93–95), the risk of proteasome and/or iProt dysfunction is high. The subsequent disruption to proteostasis could be a determining event in the loss of muscle mass and function thought to occur with obesity (1, 8–18). Considering muscle atrophy and reductions in strength amplify the risk of morbidity and mortality (13, 18, 54–58), there is much merit for future research to further delineate the specific impact obesity has on the different proteasome variants and their ability to maintain muscle proteostasis. In addition, elucidating the extent to which each individual proteasome contributes to impaired muscle proteostasis in the obese state would provide significant therapeutic opportunities. Indeed, the ability to manipulate the specific proteasome subtype with the greatest impact on obese muscle proteostasis could provide a novel mechanism to optimize the maintenance of muscle mass and thus function in obesity.

CHAPTER THREE

The Fluorometric Determination of Immunoproteasome and Total Proteasome Chymotrypsin-like Activity in Murine Skeletal Muscle: An Assay Optimization Study

Introduction

The degradation of intramuscular proteins is an essential quality control mechanism to selectively rid cells of old, misfolded, and/or damaged proteins. As muscle pathology can occur if this process is over- or under-active (1–4), cells rely on a network of regulatory systems to maintain protein homeostasis (19, 24, 111, 114–116). Although skeletal muscle contains several proteolytic mechanisms, the proteasome system is a vital component (3, 19, 25, 28, 48, 111).

Proteasomes exist in different isoforms within muscle, including the two standard proteasomes, and the less-well described immunoproteasome (iProt) (3, 22, 23). The standard proteasome system is constitutively expressed in all eukaryotic cells and comprised of two structurally similar, but functionally different variants; the 20S and 26S proteasomes. Both isoforms are large, multi-subunit complexes, which contain the 20S proteasome as their core unit (3, 22–26). Specifically, the 20S is a cylindrical protein structure consisting of four stacked heptameric rings; two identical outer alpha (α) rings, each containing seven distinct α -subunits, and two identical inner beta (β) rings with seven unique β -subunits (22, 23, 31). The β 1, β 2 and β 5 subunits are the proteolytically active components, and display caspase-like, trypsin-like and chymotrypsin-like activity, respectively. In contrast, the α rings facilitate substrate recognition (e.g., damaged proteins) and association, as well as the recruitment of regulator proteins (22, 23, 25, 26,

31). The key function of the 20S proteasome is the removal of oxidatively modified and unfolded proteins, the activity of which is enhanced when the α rings bind to an 11S regulator protein (24, 25, 29, 31). Conversely, the addition of ATP-dependent 19S regulatory complexes to both ends of the 20S core unit produces the 26S proteasome, which preferentially degrades polyubiquitinated proteins (3, 19, 24, 25, 31, 111).

Unlike the two standard proteasomes, the iProt is not constitutively expressed in muscle, but induced in situations of cellular stress (41, 46, 120, 129–131). For instance, when exposed to a pro-inflammatory stimulus (e.g., IFN- γ and TNF- α) and/or oxidative stress, the catalytic β -subunits of the standard proteasome are replaced by those of the iProt; β 1i (low molecular mass polypeptide 2 (LMP2)), β 2i (multicatalytic endopeptidase complex-like 1 (MECL-1)) and β 5i (low molecular mass polypeptide 7 (LMP7)). Such subunit substitutions slightly alters the enzymatic profile of the iProt toward enhanced chymotrypsin-like, but lower caspase-like activity (22, 23, 29, 31, 32, 120). Head-to-head comparisons show the iProt is more effective in the removal of oxidized proteins than the 20S proteasome (29, 36), and equivalent to the 26S isoform in the destruction and elimination of ubiquitinated proteins (36, 38, 39).

Accumulating research notes a disruption to 20S and/or 26S proteasome activity impairs intramuscular protein homeostasis and is associated with muscle atrophy (19, 25, 111). However, more recent evidence suggests iProt dysregulation may also be an important intermediary in muscle pathology (41, 46, 49, 120, 129–131). Consequently, the ability to quantify the proteolytic activity of the proteasome isoforms is crucial to further research in numerous atrophic disorders.

The classical and most commonly cited method for determining proteasome activity *in vitro* is through the use of fluorescently tagged peptide substrates specific for the three catalytic enzymes of the proteasome (73, 132, 133). The model peptide substrates are typically three to four amino acids in length and labeled with a fluorescent reporter molecule, such as 7-amino-4-methylcoumarin (AMC). During the assay, the sample of interest is incubated with these fluoropeptide substrates (62, 132, 133). To allow for separate quantification, specific peptide substrates are commercially available for each of the different proteasome catalytic subunits (62, 73, 132, 133). As chymotrypsin-like activity is considered rate limiting, and thus vital to protein breakdown, much research is dedicated toward the quantification of this proteasome site (62, 134, 135).

However, the ability to infer proteasome activity through the use of such model peptides alone is limited. For instance, although these substrates are preferentially cleaved by the proteasome, non-specific proteolysis by other proteases contained within the homogenate can also occur (61, 62, 73, 74). Therefore, the use of appropriate negative controls (i.e., a proteasome inhibitor) is imperative to determine proteasome-specific involvement. Of the numerous inhibitors commercially available, the peptide aldehyde MG-132 (Z-Leu-Leu-Leu-al; $C_{26}H_{41}N_3O_5$) is the most widely used (33, 48, 62, 134). Nevertheless, despite exhibiting high specificity towards proteasome inhibition, MG-132 can also inhibit other proteases within the sample (e.g., calpains and various lysosomal enzymes) in a dose-dependent manner (33, 48, 75, 76, 134). Moreover, MG-132 non-selectively inhibits all the proteasome isoforms (34, 134, 136). In contrast, the

epoxyketone ONX-0914 (PR-957; C₃₁H₄₀N₄O₇) has high specificity and selectivity for the LMP7 iProt subunit at concentrations below 300 nM (34, 137).

Regardless of the inhibitor used, the premise of the assay is the same – AMC fluorescence intensity (excitation, 340 nm; emission, 460 nm) is monitored over time with a microplate reader (62, 133). Initially, AMC fluorescence is quenched while bound to the intact substrate peptide. However, with time, proteolytic cleavage by the specific proteasome subunit present within a sample releases free AMC, and the increase in fluorescence is directly proportional to the catalytic activity of the subunit (62, 73, 132, 133). Subsequently, proteasome-specific activity, i.e., the rate of cleavage, is determined from the slope of the reaction progress curve within the linear range and compared to the slope of the negative control (i.e., the slope of the corresponding inhibitor-treated sample) (62, 133). Any non-linear portions of the reaction progress curves are excluded from the analyses (62).

Several kits for measuring chymotrypsin-like activity of the standard proteasome are commercially available (41). However, few are specific to the iProt, and those that are, were previously validated on mouse splenic samples (60), and not skeletal muscle. As the iProt content of the spleen is comparatively greater than other non-lymphoid organs (61, 73), the recommended assay conditions and inhibitor concentrations may not translate to other tissues (62), such as skeletal muscle. Consequently, we sought to trial and optimize the assay procedures listed by the manufacturer of one such kit (UBPBio, Aurora, CO) in skeletal muscle homogenate. To help guide future assays, we first sought to test a range of muscle protein concentrations to determine concentrations that yield sufficient AMC fluorescence signal intensity (i.e., signal within the mid-range of the

AMC standard curve). Lastly, dose-response trials using the ONX-0914 (iProt-specific) and MG-132 (total proteasome-specific) proteasome inhibitors were performed to test if manufacturer- and surrounding literature-recommended dosages visibly lowered chymotrypsin-like activity in skeletal muscle homogenate.

Methods and Materials

Preparation of Mouse Muscle Homogenate

Whole skeletal muscle (triceps) previously harvested from 16-week-old male wild-type mice (C57BL/6J) (Jackson Laboratories, Bar Harbor, ME) during a prior investigation (49) was used for the purpose of the current optimization study. Tissue samples were stored at -80°C until current use. All prior *in vivo* animal care and procedures were approved by the Institutional Animal Care and Use Committee (IACUC) at Baylor University.

For the present investigation, frozen triceps muscle tissue ($N = 10$) was homogenized (Polytron Kinematica, Bohemia, NY), in ice-cold cell lysis buffer (40 mM Tris, pH 7.2, 50 mM sodium chloride (NaCl), 2 mM beta-mercaptoethanol (β ME), 2 mM adenosine triphosphate (ATP), 5 mM magnesium chloride ($MgCl_2$), UBPBio, Aurora, CO). The inclusion of ATP and $MgCl_2$, and the exclusion of protease inhibitors in the lysis buffer ensured the proteasome structure, and thus activity were preserved (60, 62). Once homogenized, all samples were centrifuged at 17000 g for 20 min at 2°C. Total protein concentration contained within the muscle homogenate was determined in duplicate using the Bradford assay method, with BSA (Bio-Rad, Hercules, CA) as a standard. Homogenates were subsequently aliquoted and stored at -80°C until use.

Measurement of Intramuscular Chymotrypsin-like Activity

A commercially available fluorometric assay kit (UBPBio, Aurora, CO, cat. No. J4160) designed to measure proteasome activity *in vitro* using cell lysates or tissue extracts was used to determine chymotrypsin-like activity in triceps muscle homogenate.

AMC standard. AMC standard stock (100 μ M in dimethyl sulfoxide (DMSO), UBPBio, Aurora, CO) was diluted in assay buffer (40 mM Tris, pH 7.1 at 37°C, 2 mM β ME, UBPBio, Aurora, CO) to make a 1600 nM AMC stock standard. A two-fold serial dilution of the AMC stock standard was used to generate the standard curve (range: 1600 nM – 25 nM AMC). Blanks (0 nM AMC) were assay buffer only.

Fluorescent protease substrate. The peptide substrate Ac-ANW (Acetyl-Ala-Asn-Trp) labeled with fluorescent AMC (UBPBio, Aurora, CO) was the model substrate used to test chymotrypsin-like activity. The fluoropeptide substrate was prepared as a 50 mM stock solution in DMSO (Sigma-Aldrich, St. Louis, MO) and diluted in assay buffer (40 mM Tris, pH 7.1 at 37°C, 2 mM β ME, UBPBio, Aurora, CO) to a final concentration of 100 μ M immediately prior to use.

Proteolysis assay – determining sample protein concentrations that yield suitable fluorescence within the range of the standard curve. Muscle homogenates ($N = 10$) were diluted in assay buffer (40 mM Tris, pH 7.1 at 37°C, 2 mM β ME, UBPBio, Aurora, CO) to final concentrations of 1 mg ($n = 1$), 3 mg ($n = 5$) and 5 mg ($n = 4$). The protein concentrations selected were based on assay recommendations to plate samples in a final concentration between 1 – 5 mg protein. Diluted samples were subsequently incubated in assay buffer for 10 min at 37°C prior to fluoropeptide substrate addition. A serial dilution

of AMC (UBPBio, Aurora, CO) was used to generate a standard curve. Sample chymotrypsin-like activity was measured by monitoring AMC liberation over time with a multi-mode microplate reader (Varioskan LUX, Waltham, MA) using excitation and emission wavelengths of 340 nm and 460 nm, respectively. All experiments were performed at 37°C in a final volume of 100 μ L (50 μ L sample and 50 μ L Ac-ANW-AMC (100 μ M) substrate) in black, 96-well microtiter plates (Greiner Bio-One, Monroe, NC). AMC fluorescence was measured every minute for 15 min, and the microplate reader was programmed to probe from the top of the plate and shake for 5 s immediately prior to each reading. All assays were performed in triplicate, with blank values subtracted. As the purpose of this trial was to compare the fluorescence of samples containing different concentrations of protein against that of the AMC standard curve, negative controls (proteasome inhibitors) were not required.

Proteasome inhibitor selection and stock preparation. Two proteasome inhibitors were used for the purpose of our optimization trials; 1) MG-132, supplied with the assay kit, and 2) ONX-0914 (UBPBio, Aurora, CO, cat. No. F1410). Although Ac-ANW-AMC is a preferred substrate of the iProt, cleavage can also occur via the standard proteasome, albeit at a reduced rate (approximately 6-fold slower when compared to the iProt) (60, 138). Consequently, the ONX-0914 inhibitor was selected to test iProt-specific enzymatic activity. MG-132 was included as a measure of total proteasome activity. Additionally, the *in vitro* use of MG-132 was previously validated in proteasomes extracted from rodent skeletal muscle (46, 129, 139), and thus we elected to include MG-132 to be consistent with the body of literature. MG-132 and ONX-9014 were prepared as 10 mM

and 25 μM stock solutions in DMSO (Sigma-Aldrich, St. Louis, MO), respectively. Stock solutions were stored as aliquots at -80°C until use.

Selection of proteasome inhibitor dose range. Inhibitor concentrations were selected based on proprietor recommendations and the surrounding literature. Prior investigations note a 200 μM concentration of MG-132 is sufficient to inhibit activity in proteasomes extracted from muscle tissue lysates (46, 129, 139). However, recommended *in vitro* concentrations are 50-200 μM (UBPBio, Aurora, CO). Consequently, eight different MG-132 concentrations within, and slightly beyond, the recommended range were selected for dose-response assays (i.e., 60, 80, 100, 125, 160, 200, 250 and 315 μM). Concentrations selected were equally spaced on a log-based scale.

No comparable data for the *in vitro* inhibition of the iProt in skeletal muscle was available. Therefore, ONX-0914 dosage selection was based on: 1) typical dose ranges for *in vitro* assays stated on the data sheet (i.e., 100 – 500 nM), 2) concentrations previously utilized and validated in other tissue lysates (200 nM) (34), and 3) per assay manufacturer recommendations (optimally 200 nM, but no more than 300 nM). Eight dosages of ONX-0914, with concentrations increasing on a log-scale, were subsequently selected (i.e., 100, 125, 160, 200, 250, 315, 400 and 500 nM) for the dose-response trials.

Proteolysis assay – dose-response trials. Prior to fluoropeptide (Ac-ANW-AMC) substrate addition, the muscle homogenate (3 mg) was pre-incubated in assay buffer (40 mM Tris, pH 7.1 at 37°C , 2 mM βME , UBPBio, Aurora, CO) for 10 min at 37°C in the absence or presence of varying concentrations of ONX-0914 or MG-132. Due to limited sample availability, the dose-response curves were only tested on one sample. Peptidase

activity was measured by monitoring AMC liberation over time as previously described using excitation and emission wavelengths of 340 nm and 460 nm, respectively. The dose-response trial was performed at 37°C in a final volume of 100 uL in black, 96-well microtiter plates (Greiner Bio-One, Monroe, NC), and AMC fluorescence was measured every minute for 15 min. The ONX-0914 assays were performed in triplicate; however due to sample volume limitations, the MG-132-treated samples were performed in duplicate. Relative AMC fluorescence readings (fluorescence with blank values subtracted) measured over time were subsequently plotted in Microsoft Excel (Microsoft Office Professional Plus 2019, version 2104) to generate dose-response curves. Conclusions regarding optimal inhibitor concentrations to use for future investigations were based on: 1) the visual assessment of the dose-response curves at the final fluorescent reading (i.e., the reading at 15 min), 2) manufacturer suggestions, and 3) the surrounding literature.

Statistical Analyses

All graphics and linear trendline correlation computations were generated in Microsoft Excel (Microsoft Office Professional Plus 2019, version 2104). SPSS (version 26.0) for Windows was used to perform statistical analyses. Statistical significance was accepted at the $p < .05$ level of confidence. One-way analysis of variance (ANOVA) and Bonferroni post-hoc tests were used to compare change in AMC fluorescence intensity in muscle homogenate containing varying amounts of total protein. All values are reported as mean \pm standard error of the mean (SEM) where appropriate. Conclusions regarding

optimal assay inhibitor concentrations were based on the visual assessment of the data, manufacturer suggestions and the surrounding literature.

Results

AMC Fluorescence in Relation to Muscle Homogenate Protein Content

The initial purpose of the assay optimize trials was to determine muscle sample protein concentrations which yield AMC fluorescence signal intensity within the range of the AMC standard curve. A serial dilution of AMC was used to generate a standard curve for comparative purposes (figure 3.1). The resulting trendline illustrates fluorescence intensity is proportional to the concentration of free AMC in assay buffer ($R^2 = .9999$). The range of AMC fluorescence (i.e., mean AMC fluorescence of the replicates) between the low (25 nM) and high (1600 nM) standards was $4.31 \pm .02$ AFU and 138.00 ± 1.40 AFU, respectively (blank fluorescence was $2.25 \pm .03$ AFU).

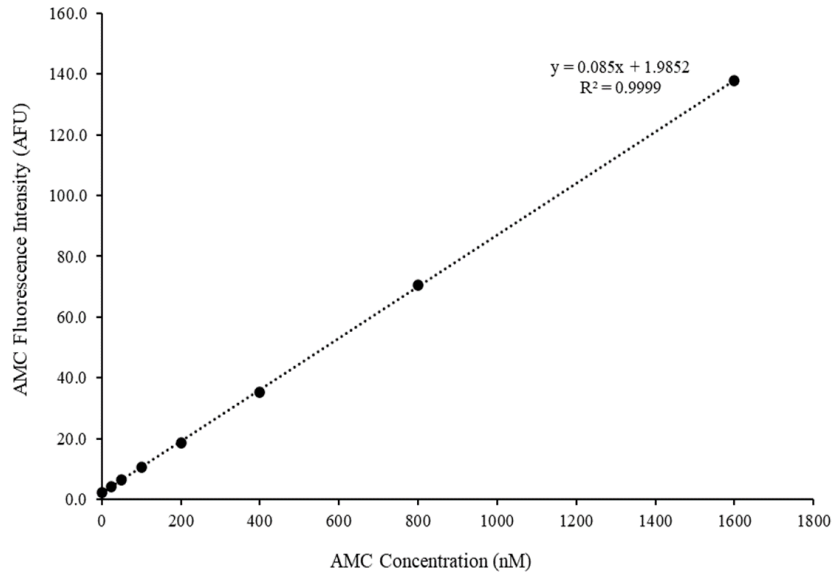


Figure 3.1. AMC standard curve. Data points are mean AMC fluorescence intensity as a function of AMC concentration within the assay buffer. Standards were plated in duplicate. The trendline equation and associated R^2 value are also displayed.

AMC fluorescence intensity liberated over time from skeletal muscle homogenates of varying final concentrations (1 mg, 3 mg, and 5 mg) are displayed in figure 3.2. When samples containing 3 mg and 5 mg protein were compared, one-way ANOVA with post-hoc tests revealed samples containing 5 mg protein liberated a significantly greater fluorescence signal across all time points of the reaction progress curve ($p < .001$ for all comparisons). Nevertheless, samples containing 3 mg and 5 mg protein both produced fluorescence signals within the range of the AMC standard curve. In contrast, muscle homogenate containing 1 mg protein yielded a weak signal, which was significantly lower than samples containing 3 mg from the third minute of the reaction (3 mg protein $5.31 \pm .1$ RFU vs 1 mg protein $3.21 \pm .1$ RFU, $p = .040$), and lower than 5 mg protein across all time points of the reaction progress curve ($p < .001$ for all comparisons)

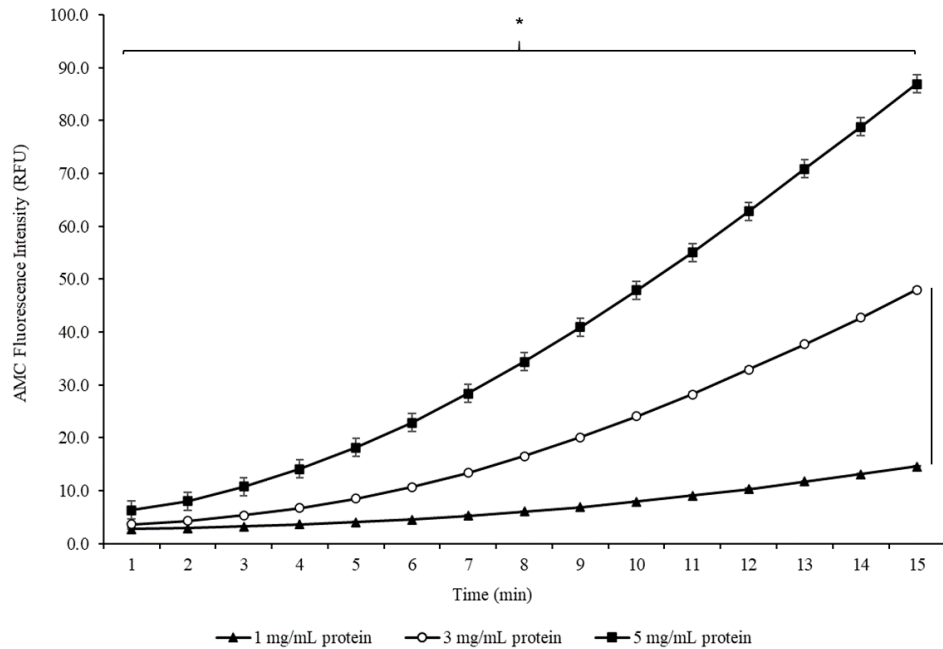


Figure 3.2. Intensity of AMC fluorescence liberated from skeletal muscle homogenates of varying protein concentrations. Data are displayed as mean AMC fluorescence with blank values subtracted \pm SEM for samples containing 3 mg ($n = 5$) and 5 mg ($n = 4$) protein, respectively. Data for the sample containing 1 mg protein ($n = 1$) are displayed as mean fluorescence of replicates with blank values subtracted \pm SEM of the replicates. All samples were plated in triplicate for this trial. A one-way ANOVA with Bonferroni post-hoc tests revealed * samples containing 5 mg protein produced significantly greater signal compared to samples containing 3 mg and 1 mg protein across all time points ($p < .001$ for all comparisons), and † fluorescence intensity for samples containing 3 mg protein was significantly greater than 1 mg protein from the third minute of the reaction progress curve ($p < .050$ for all remaining comparisons).

Dose-Response Trials

AMC fluorescence liberated from skeletal muscle homogenate (3 mg, $n = 1$) in the absence or presence of varying concentrations of ONX-0914 or MG-132 are displayed in figures 3.3 and 3.4, respectively. All concentrations of the proteasome inhibitors yielded visibly lower AMC fluorescence at each time point, when compared to untreated homogenate. Upon visual assessment of the final fluorescence reading (i.e., the reading at 15 min), the reduction in AMC fluorescence appeared to cluster for ONX-0914-treated homogenates between a concentration of 160 – 400 nM. For homogenate

treated with MG-132, fluorescence reduction clustered between 125 – 200 μ M. Such visual, mid-range “clustering” of fluorescence is suggestive of optimal dose ranges for proteasome-specific inhibition (per communication).

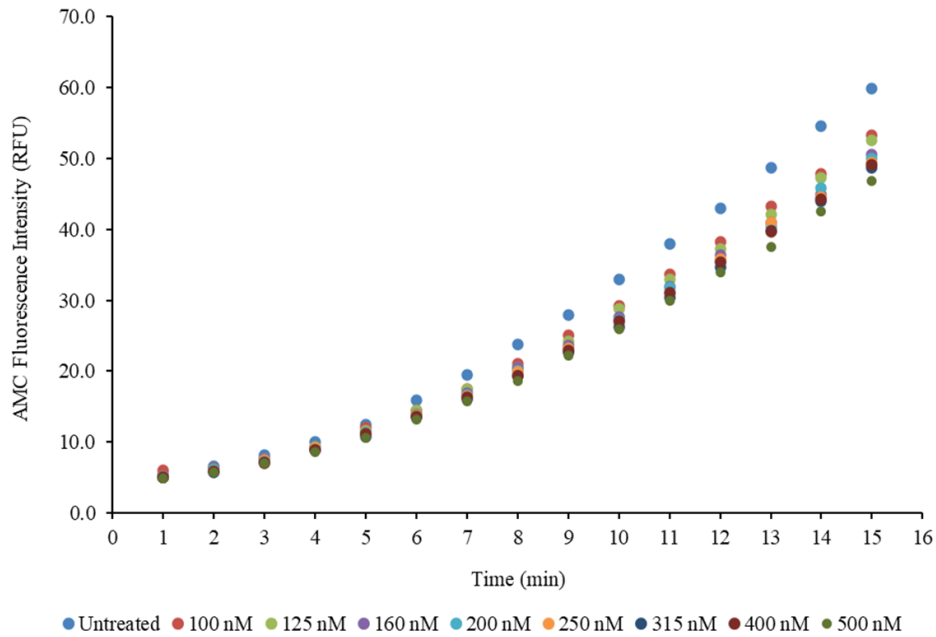


Figure 3.3. Intensity of AMC fluorescence liberated from skeletal muscle homogenate (3 mg protein) in the absence and presence of varying doses of the iProt inhibitor ONX-0914. Data are displayed as mean AMC fluorescence with blank values subtracted.

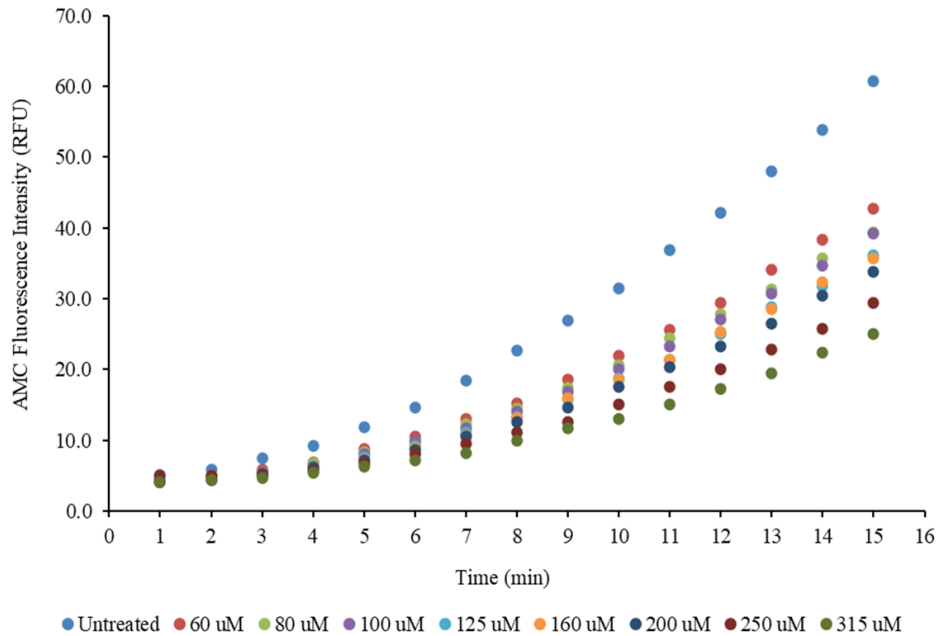


Figure 3.4. Intensity of AMC fluorescence liberated from skeletal muscle homogenate (3 mg protein) in the absence and presence of varying doses of the non-specific proteasome inhibitor MG-132. Data are displayed as mean AMC fluorescence with blank values subtracted.

Discussion

Although several kits for measuring chymotrypsin-like activity of the proteasome are commercially available (41), few are specific to the iProt. Moreover, many of the available assays require proteasome extraction and purification prior to use and are unsuited for the direct assessment of proteolytic activity in tissue homogenate (62, 135, 140). The process of extraction involves tissue and cell lysis (either via sonication, glass bead disruption, freeze thaw lysis or via the use of detergents), centrifugation and washing. Such procedures are costly, time consuming, typically require large numbers of cells and may ultimately interfere with proteasome activity (62, 135). Despite the recent development of fluorometric assays appropriate for use with tissue homogenate (60, 135), their utility in murine skeletal muscle was unknown. Consequently, the present study

sought to trial and optimize the assay procedures listed for a kit previously deemed suitable for the *in vitro* assessment of chymotrypsin-like activity in tissue homogenate (60).

Considering the relatively small size of murine limb muscles, muscle homogenate sample volumes are invariably low. Given these restrictions and the large volumes required to perform the assay, the purpose of the initial trial was to assess a range of muscle protein concentrations to determine the minimal protein content that would yield sufficient AMC fluorescence signal intensity. Establishing these concentrations were essential to guide future analyses. As the suggested final protein concentrations for the assay were between 1 – 5 mg protein, and due to the limited number of samples available, we elected to test muscle homogenate containing 1 mg, 3 mg and 5 mg protein. Our results show that once the reaction progress curves achieved linearity, sample concentrations containing 3 mg and 5 mg protein produced AMC fluorescence within an appropriate range of the standard curve. In contrast, the signal was comparatively weak for samples containing 1 mg protein. Future studies should therefore ensure final protein concentrations for the assay are maximized as much as possible to achieve optimal fluorescence. Nevertheless, we clearly demonstrate 3 mg protein produces sufficient signal that would enable the further calculation of proteasome activity (by extrapolation to the standard curve) (62).

Hence, muscle homogenate containing 3 mg protein was utilized for the dose-response trials¹. The subsequent data show all doses of the inhibitors assessed produced visibly lower AMC fluorescence, when compared to untreated muscle homogenate.

¹ Sample volumes allowed for the use of 3.5 mg protein for the study described in Chapter Four.

However, selecting optimal proteasome inhibitor concentrations for use in future assays is inherently complicated given both MG-132 and ONX-0914 lose inhibition specificity at high concentrations (33, 34, 48, 62, 75, 76, 134, 137). For instance, although MG-132 is a potent inhibitor of the proteasome, co-inhibition of other proteases contained within the sample, such as calpains and various lysosomal enzymes, can also occur in a dose-dependent manner (33, 48, 75, 76, 134). Similarly, the iProt-specific inhibitor ONX-0914 is suggested to lose specificity and inhibit all proteasome isoforms at concentrations exceeding 300 nM (34, 137). As a result, conclusions regarding optimal inhibitor concentrations, which also minimize the risk of non-specific inhibition, were based on: 1) the visual assessment of the data, 2) manufacturer suggestions and 3) the surrounding literature. First, per manufacturer recommendation, the reaction progress curves generated during the dose-response trials were visually evaluated for patterns (“clusters”) in the data. Specifically, a visual assessment of the final fluorescence reading (i.e., the reading at 15 min) was performed to determine inhibitor concentrations which “clustered”, or liberated a similar mid-range lowering of AMC fluorescence intensity. Our graphics show, inhibitor-treated muscle samples appeared to yield comparable reductions in AMC fluorescence intensity between doses of 160 – 400 nM (ONX-0914), and 125 – 200 μ M (MG-132). However, as the risk of non-specific proteasome inhibition increases when ONX-0914 concentrations exceed 300 nM (34, 137), and since a dose of 200 nM was previously shown to produce optimal iProt inhibition in other tissue samples (34), we propose 200 nM as the most appropriate option for future research with skeletal muscle.

For MG-132 sample treatment, prior investigations note a 200 μM dose inhibits chymotrypsin-like activity in proteasomes extracted from rodent skeletal muscle tissue lysates (46, 129, 139). Therefore, the observations of our preliminary trials, together with the body of literature suggests 200 μM MG-132 is sufficient for the *in vitro* inhibition of proteasomes contained within muscle homogenate, while also minimizing the risk of non-specific protease inhibition bias.

Conclusions

Considering the above conclusions are largely based on observational analyses and assumptions, this work is not without limitations. Nevertheless, given the combined evidence available, we believe the present study demonstrates measures future investigations can take to optimize assay conditions for murine skeletal muscle. Future work should also consider the between-sample variability in proteasome concentration when estimating proteasome activity. Although such measures were not required to satisfy the specific aims of the current preliminary trials, future experimental studies should normalize estimates of proteasome activity to the total proteasome content contained within each tissue sample to ensure results are comparable (33, 73).

CHAPTER FOUR

Obesity-induced Alterations to the Immunoproteasome: A Potential Link to Impaired Proteostasis in Skeletal Muscle

Introduction

Obesity can reduce muscle mass and strength (1, 8–18), and the incidence of adverse health outcomes including future disability, morbidity and mortality, is greatly amplified when these risk factors present together (13, 141–143). Growing evidence suggests obesity creates an increasingly toxic intramuscular environment, which can be highly damaging to muscle cells and cellular molecules (15, 20, 27). Due to their relative abundance, intramuscular proteins are prime targets (27, 37), and a disruption to protein homeostasis (proteostasis) is a likely determining event in the loss of muscle integrity and function thought to occur with obesity (8, 10, 12, 15, 19, 20). Although chronic inflammation and oxidative stress contribute to impaired proteostasis, the underlying mechanisms which coordinate subsequent obese muscle pathology are unclear (8, 12, 19). Nevertheless, proteasomes may play a crucial role (21).

The standard 20S and 26S proteasome systems are major cellular pathways responsible for protein degradation (3, 22–26), and essential to prevent the toxic accumulation of damaged, modified (e.g., oxidized), defective and/or partially unfolded proteins (19, 24, 27, 28) - a hallmark of compromised proteostasis (20, 27, 28). Through these systems, polyubiquitinated and oxidatively modified proteins are degraded via the 26S or 20S proteasomes, respectively (3, 22–26, 28, 29). However, in the presence of oxidative stress or a pro-inflammatory stimulus, the catalytic subunits of the standard

proteasomes ($\beta 1$, $\beta 2$ and $\beta 5$) are replaced by the inducible subunits of the immunoproteasome (iProt); $\beta 1i$ (low molecular mass polypeptide 2 (LMP2)), $\beta 2i$ (multicatalytic endopeptidase complex-like 1 (MECL-1)) and $\beta 5i$ (low molecular mass polypeptide 7 (LMP7)) (22, 23, 29–33). When compared to the standard proteasome, the iProt displays enhanced chymotrypsin-like, but lower caspase-like catalytic activity (22, 23, 29, 31, 32, 120). This slightly altered enzymatic profile allows for distinct functions such as antigen presentation, T-cell differentiation and cytokine production (21, 22, 30, 33, 34). Consequently, the iProt is considered an important regulator of the immune response (21, 22, 30, 33, 34). However; additional, standard proteasome-analogous functions were recently revealed, such as the degradation of both oxidized and polyubiquitinated intracellular proteins (22, 23, 31, 35). Moreover, within pro-inflammatory and/or pro-oxidant environments, iProt upregulation exceeds the 20S proteasome (22, 29, 31, 37), and the 26S proteasome system is transiently inactivated (23, 28, 31, 38, 39). Head-to-head comparisons also show the iProt is more effective than the 20S proteasome in removing oxidatively damaged proteins (29, 36), and is at least as efficient, if not more efficient, than the 26S proteasome in the destruction and elimination of ubiquitinated proteins (36, 38, 39). This evidence suggests the iProt has a vital role in sustaining proteostasis, particularly under conditions of inflammation and oxidative stress (29, 31, 37–39).

The iProt may also have muscle-specific functions (40) as iProt suppression promotes intracellular protein oxidation and prevents muscle differentiation in both murine and human skeletal muscle myoblasts (41). Conversely, skeletal muscle concentrations of the LMP7 subunit are increased in several inflammation/oxidative

stress-associated atrophic disorders, such as aging sarcopenia (42, 43), denervation (46), muscular dystrophy (44, 45), and idiopathic inflammatory myopathies (47). Although the pathological significance of raised LMP7 cannot be inferred from intramuscular concentrations alone (35, 48), the above data suggest the iProt may aid the maintenance of muscle mass, and may become dysregulated in situations of chronic inflammation and/or oxidative stress.

Whether the iProt is altered within obese muscle is currently unclear.

Nevertheless, a preliminary study conducted in our lab found 12-weeks of high-fat feeding significantly increased both oxidative stress (lipid peroxidation) and protein concentrations of the LMP7 subunit in the gastrocnemius (GA) muscle of wild-type (C57BL/6J) mice. In contrast, intramuscular inflammation (pro-inflammatory macrophages) and the concentration of the MECL-1 iProt subunit were unaffected by diet-induced obesity (DIO) (49). While the increase in the LMP7 subunit could represent a compensatory mechanism to clear oxidatively damaged proteins and regain cellular homeostasis (22, 23, 31, 32), accumulating evidence suggests oxidized proteins tend to aggregate under conditions of chronic oxidative stress (31, 35). Previous research investigating the impact of cellular aging on the standard 20S proteasome demonstrates that while oxidized protein aggregates retain the ability to bind to the outer (i.e., alpha) subunits of the proteasome, these proteins are often too large to enter the catalytic core (50–52). Consequently, further protein aggregation occurs, which may ultimately result in proteasome sequestration-induced inhibition (27, 50, 51, 53). Although iProt enzymatic activity was not assessed in our previous study (49), the alpha-subunits of the iProt and standard proteasomes are structurally identical (23, 31, 35). Thus, the increase

in muscle LMP7 content noted in the obese mice of our prior investigation could conceivably represent inactive or inhibitor-bound units. Considering LMP7 is also required for the post-translational processing and maturation of the LMP2 and MECL-1 iProt subunits (22, 31, 35), such a protein aggregate-induced reduction in LMP7 activity may also explain why intramuscular concentrations of the MECL-1 subunit were unaltered by DIO despite a rise in LMP7 content (49). If iProt activity is impaired in obesity, the subsequent inability to contain oxidatively damaged protein aggregation (i.e., maintain proteostasis) could ultimately predispose obese individuals to reductions in muscle mass and/or function. As low muscle mass and strength are important predictors of future functional independence, morbidity and mortality (13, 18, 54–59), there is a need to determine potential regulators of muscle proteostasis and how these factors may or may not be altered in the obese state.

Therefore, the purpose of the present study was to extend the investigations of our prior work (49). Specifically, the current investigation sought to elucidate the impact of an obesogenic diet (high-fat, high-sucrose) on 1) intramuscular iProt content and activity, and 2) whether any alterations to the iProt were associated with intracellular oxidized protein (i.e., protein carbonyl) accumulation in wild-type (WT) mice. Although our previous study saw no change in markers of pro-inflammatory macrophages within the muscle of obese mice, intramuscular cytokines were not analyzed. As interferon-gamma (IFN- γ) and tumor necrosis factor-alpha (TNF- α), are considered the most robust pro-inflammatory activators of the iProt (22, 23, 31), and since local inflammation within obese muscle is conflicting (9, 83), a further aim of the present study was to assess protein concentrations of these cytokines in the muscle of WT mice with and without

DIO. Lastly, although we previously noted high-fat feeding caused a significant reduction in GA muscle mass when expressed relative to total body mass, absolute muscle mass was increased, thus rendering the significance of the former findings unclear (49). However; obesity-associated reductions in muscle contractile function and relative strength (13, 17, 18) are currently considered stronger predictors of future adverse health outcomes (17, 18, 59, 79, 80) and typically manifest prior to a change in muscle mass (59). As strength could be negatively impacted by possible iProt dysfunction, and was not measured in our prior study, a final aim of the current investigation was to confirm the effect of HFS-feeding on muscle strength in WT mice (81, 82). The impact of DIO on absolute and relative muscle mass was also assessed.

We hypothesized intramuscular concentrations of the iProt subunits, protein carbonyls, IFN- γ and TNF- α would be increased, however; iProt activity, and body mass-adjusted strength and muscle mass would be reduced in mice with DIO.

Methods and Materials

Animals

Four-week-old male wild-type mice (C57BL/6J) (initial $N = 24$) (Jackson Laboratories, Bar Harbor, ME) were housed (4 mice per cage) and treated in the Animal Research Facility at Baylor University. The mice were acclimated to the facility for 7 days prior to any experimental sessions. All mice were housed on a 12:12h light-dark cycle with access to food and water ad libitum. Animal care and procedures were approved by the Institutional Animal Care and Use Committee (IACUC) at Baylor University.

Experimental Groups

Following acclimation, study animals were randomized into two diet groups; half ($n = 12$) were fed a high-fat, high-sucrose (HFS) diet consistent with the typical western diet (66), and the remainder a low-fat, low-sucrose control (LFS) diet. However, due to excessive fighting, one mouse assigned to the LFS diet group required humane euthanasia during the first week of feeding (final LFS group $n = 11$). The feeding phase of the study occurred over a 12-week duration to be consistent with the timeline of our prior investigation (49). Online statistical computing web programming (www.randomization.com) was used to generate the randomization schedule for this study. Individual animal cages were assigned to the respective diet groups by a member of Baylor's Veterinary Care Staff who was blinded to the study hypotheses.

Sample Size Estimations

The number of proposed mice per experimental group was determined by a sample size estimation for a two-tailed independent t-test. The main effects of interest were the mean difference in; 1) iProt content and activity and 2) protein carbonylation and inflammation within skeletal muscle, as well as 3) the mean difference in muscle mass and strength in mice. As measures of protein carbonyls and muscle strength were not analyzed in our prior study, and effect size estimates were unavailable from the surrounding literature, sample size for the current investigation was calculated based on effect size estimates for the variables LMP7 (*Cohen's* $d = 3.4$), intramuscular lipid peroxidation (8-isoprostane, *Cohen's* $d = 2.6$) and relative muscle mass (*Cohen's* $d = 1.24$) (49). To ensure optimal power, final sample size was determined using the effect size for change in relative muscle mass. Therefore, a power analysis for a two-tailed

independent t-test (G*Power, version 3.1.9.4) using an effect size of 1.24, revealed a sample size of $n = 12$ mice per experimental group was sufficient to find an alpha of .05 with a power of .80 (actual power = .83). Due to animal attrition in the first week of feeding, power was re-estimated using the same effect size. These estimations revealed the loss of one animal in the LFS diet group would not reduce power substantially (power = .81). Lastly, owing to the larger effect size estimates for the variables LMP7 and 8-isoprostane, a sub-set of muscle samples were selected for biochemical analyses.

Although a sample size estimate for an independent t-test using an effect size of 2.6, showed 4 muscle samples per experimental group would provide adequate power, a minimum of $n = 8$ samples per group were used (actual $n = 8-12$ depending on the nature and delimitations of each individual assay). The muscle sample sub-sets were selected at random within each diet group.

Animal Diet and Assessment of Food Intake and Body Mass

Starting at 5-weeks of age, mice were either fed a high-fat, high-sucrose (45% kcal fat, 17% sucrose), or a low-fat, low-sucrose (10% kcal fat, 0% sucrose) chow diet (Open Source Diets, New Brunswick, NJ). The experimental feeding period was 12-weeks in duration, a timeline sufficient to induce a significant divergence in body mass between the control and obese groups (63, 66, 85). Except for fat and sucrose, both diets were matched for overall ingredient content. Food was replaced, and intake measured every second day. Based on standard adult mouse food requirements (144), both groups received the same pre-weighed amount of chow (4 g/day), multiplied by the number of mice per cage. The quantity of chow consumed per cage was determined by subtracting

the weight of remaining food from the pre-weighed amount of feed initially given (49). All mice were weighed bi-weekly to assess for changes in body mass.

Assessment of Blood Glucose

Blood glucose was assessed on four separate occasions; a baseline measure of glycemia was determined in all mice at the onset (i.e., first day) of the feeding phase, with subsequent analyses conducted once every four weeks until euthanasia at the beginning of week 13. Whole blood was sampled via tail-tip amputation following a 5 h (morning) fast (145) and blood glucose concentrations were determined using a handheld whole-blood glucose monitor (OneTouch Ultra2, Lifescan, Malvern, PA).

Assessment of Forelimb Muscle Strength

Muscle strength was assessed via the forelimb weight lifting test. This test is a valid and reproducible assessment of forelimb strength (81, 82), which exploits a mouse's natural instinct to readily and strongly grasp onto small, thin wire mesh balls (weighing 7 g) connected to a series of steel chain links (13 g each) (81). Briefly, the test measures the maximal weight a mouse can lift with their forepaws using a series of seven progressively heavier weights, each connected to a small wire mesh ball (weighing 20, 33, 46, 59, 72, 85 and 98 g, which corresponds to the number of links attached to each wire ball). For each trial, mice were held mid-tail and lowered toward the wire ball. Maintaining grip for 3 s was the criterion for a successful lift, and mice were allowed three attempts at each weight, with 10 s rest between attempts. Three failed attempts at a specific weight were grounds for test termination. Individual mice were assigned a final strength score based on the maximum time and weight achieved (16, 81, 82). For example, a mouse

successfully lifting the first three chain weights for 3 s each, but dropped the four-link chain after 1 s on its final attempt, received a strength score of 10 ($[(3 \text{ sec criterion achieved} * \text{ number of links}] + \text{ time attempted to hold next heavier weight in the series})$, i.e., $= 3 \times 3 + 1$) (81, 82). Both absolute strength scores, and scores normalized to test-day body mass (16) are reported. Although this test is an assessment of forelimb strength, and muscles harvested for biochemical analyses were hindlimb muscles, to avoid potential bias, week 11 was selected as the time point for performing strength assessments in preference to week 12.

Animal Euthanasia and Tissue Collection

The animals were euthanized by cervical dislocation while under a heavy plane of gaseous anesthesia. Tissues harvested included; skeletal muscle and epididymal fat pads (i.e., visceral white adipose tissue). As fast-twitch muscle is more susceptible to lipid-induced stress and accumulation (67, 68), and to minimize possible muscle fiber type-related bias in our results, type II fiber predominant muscles (white gastrocnemius (GA) and tibialis anterior (TA) muscle) (69, 70) were selected for the purpose of this study. Additionally, as DIO may affect weight-bearing (e.g., GA) and non-weight bearing (e.g., TA) muscle groups differentially (18, 71), both the GA and TA muscle groups were harvested and included in subsequent analyses for comparative purposes. Once dissected, individual muscles were rinsed in PBS, trimmed of any attached adipose tissue, weighed and snap frozen in liquid nitrogen. The left GA and TA muscles were used to assess protein concentrations of our markers of interest, and the right GA and TA muscles were used for the assessment of iProt activity. The epididymal fat pad weight was used as a proxy for central adiposity and to confirm obesity status (146). All tissue sample tubes

were labeled with a unique serial number to blind investigators involved in endpoint analyses and stored at -80°C until use.

Muscle Preparation for ELISA Assays

As protease inhibitors may alter the proteasome, frozen GA and TA muscle tissue was homogenized (Polytron Kinematica, Bohemia, NY) in ice-cooled PBS alone and stored overnight at -20°C ($n = 8$ GA samples per diet group, $n = 11$ and $n = 12$ TA samples in LFS and HFS diet groups, respectively). Following two freeze-thaw cycles, the muscle homogenates were centrifuged at 5000 g for 5 min at 4°C per ELISA kit manufacturer recommendations. Total protein concentration contained within the homogenate was determined in duplicate using the Bradford assay method, with BSA (Bio-Rad, Hercules, CA) as a standard. Homogenates were then be aliquoted and stored at -80°C until use.

Quantification of Intramuscular iProt, Total Proteasome and Inflammatory Cytokine Content

Commercially available ELISA kits were used to determine protein concentrations of; the catalytic iProt subunits (LMP2, LMP7 and MECL-1), the α -7 proteasome subunit (total proteasome content), and the cytokines IFN- γ and TNF- α (MyBioSource, San Diego, CA). All assays were read at a wavelength of 450 nm using a microplate reader (xMark, Bio-Rad, Hercules, CA) against a known standard. Measurements were performed in duplicate and normalized to the total protein content of the muscle homogenate. Final concentrations of the iProt subunits were also expressed relative to the total proteasome content contained within each sample as previously described (42, 43, 46, 120).

Quantification of Intramuscular Oxidative Stress (Protein Carbonyls)

Protein carbonyl concentration was assessed in GA and TA muscle homogenate using the OxiSelect™ Protein Carbonyl ELISA Kit (Cell Biolabs, Inc., San Diego, CA) per the manufacturer's instructions. All assays were performed in duplicate, read at a wavelength of 450 nm using a microplate reader (xMark, Bio-Rad, Hercules, CA), and final concentrations were normalized to the total protein content of the muscle homogenate.

Muscle Homogenate Preparation for Proteasome Activity Assays

Frozen GA and TA muscle tissue ($n = 8$ GA and TA samples per diet group) were homogenized (Polytron Kinematica, Bohemia, NY), in ice-cold cell lysis buffer (40 mM Tris, pH 7.2, 50 mM NaCl, 2 mM β ME, 2 mM ATP, 5 mM $MgCl_2$, UBPBio, Aurora, CO). The inclusion of ATP and $MgCl_2$, and the exclusion of protease inhibitors in the lysis buffer ensured the proteasome structure, and thus activity were preserved (60, 62). Following centrifugation at 17000 g for 20 min at 2°C (60), total protein concentration contained within the muscle homogenate was determined in duplicate using the Bradford assay method, with BSA (Bio-Rad, Hercules, CA) as a standard. Homogenates were subsequently aliquoted and stored at -80°C until use.

Quantification of Intramuscular Proteasome Activity

Chymotrypsin-like activity in GA and TA muscle homogenate was determined via a Fluorometric Assay Kit (UBPBio, Aurora, CO). The assay protocol was optimized for use in skeletal muscle homogenate as described in Chapter Three. Briefly, the peptide substrate Ac-ANW labeled with fluorescent AMC (7-amino-4-methylcoumarin) was the

model substrate used to test chymotrypsin-like activity. The fluoropeptide substrate was prepared as a 50 mM stock solution in DMSO and diluted in assay buffer (40 mM Tris, pH 7.1 at 37°C, 2 mM β ME, UBPBio, Aurora, CO) to a final concentration of 100 μ M. Prior to fluoropeptide addition, muscle homogenates (3.5 mg) were pre-incubated in assay buffer for 10 min at 37°C in the absence or presence of the iProt-specific inhibitor ONX-0914 (200 nM), or MG-132 (200 μ M), a non-specific proteasome inhibitor. Due to the large sample volumes required, MG-132 analyses were only performed in GA muscle homogenate. A serial dilution of AMC (UBPBio, Aurora, CO) was used to generate a standard curve. Peptidase activity was measured by monitoring AMC liberation over time with a multi-mode microplate reader (Varioskan LUX, Waltham, MA) using excitation and emission wavelengths of 340 nm and 460 nm, respectively. All experiments were performed at 37°C in black, 96-well microtiter plates (Greiner Bio-One, Monroe, NC), and AMC fluorescence was measured every minute for 15 min per manufacturer's instructions. All assays were performed in triplicate, with negative control (i.e., inhibitor-treated samples) and blank values subtracted. Mouse spleen extracts (UBPBio, Aurora, CO) served as a positive control. The rate of chymotrypsin-like activity was determined by comparing peptide fluorescence from inhibitor-treated and untreated samples (within the linear range of the kinetic curve), with AMC fluorescence of the standard curve (43, 46, 60). Enzyme activity was subsequently normalized to the total proteasome content (i.e., the α -7 subunit) contained within each tissue sample to ensure activity measures were comparable between samples (46, 61, 62, 73, 74). Normalized activity measures are presented as nmol AMC liberated per minute per mg protein, per ng/mg of the α -7 subunit (nmol/ng/min).

Statistical Analyses

SPSS (version 26.0) for Windows was used to perform the statistical analyses. Significance was accepted at the $p < .05$ level of confidence. Change in body mass and blood glucose between normal-weight and obese mice during the feeding period was assessed via a mixed model analysis of variance (ANOVA) and post-hoc tests consisting of pairwise comparisons with Bonferroni correction. One-tailed statistical tests were used to compare group differences in confirmatory variables. Specifically, one-tailed independent t-tests were used to compare strength scores between LFS-fed and HFS-fed mice, however; a Mann-Whitney-U test was required to compare epididymal fat mass (due to non-normal data). Between diet-group comparisons of all other variables at study completion were analyzed via two-tailed statistical tests. Independent t-tests were used to compare GA and TA muscle mass, muscle concentrations of LMP2, LMP7, MECL-1, protein carbonyls, IFN- γ , TNF- α and muscle chymotrypsin-like activity. Due to lack of normality, a Mann-Whitney-U test (two-tailed) was used to compare between group differences in GA and TA muscle total proteasome content (i.e., the α -7 subunit). All values are reported as mean \pm standard error of the mean (SEM).

Results

Body Mass, Epididymal Fat Mass and Skeletal Muscle Mass

Animal body mass did not differ (HFS $17.6 \pm .6$ g vs LFS $16.4 \pm .7$ g, $F(1,21) = 1.87$, $p = .186$) between the two experimental diet groups at study initiation. However, mice fed the HFS diet demonstrated a significantly greater body mass (HFS $20.57 \pm .5$ g vs LFS $17.4 \pm .5$ g, $F(1,21) = 22.82$, $p < .001$) within the first week of high-fat, high-

sucrose feeding. The significant divergence in body mass between obese and control groups continued for the remainder of the feeding period ($p < .001$ for all subsequent time points) (figure 4.1). At study completion, HFS- and LFS-fed mice gained 135% and 64% of their initial body mass, respectively, and epididymal fat mass was significantly greater ($U = 0.00, p < .001$) in mice fed the HFS diet (Table 4.1).

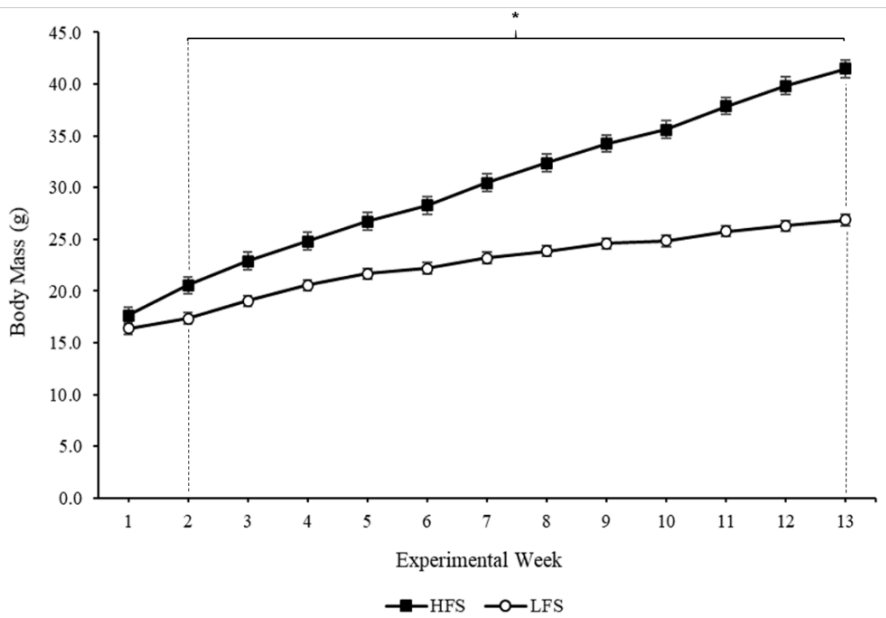


Figure 4.1. Change in body mass with high-fat, high-sucrose feeding. A mixed method (2x13) ANOVA and pairwise comparisons using Bonferroni adjustment were used to compare weekly change in body mass between LFS- and HFS-fed mice over the experimental feeding period. Data are displayed as mean \pm SEM at each time point and * denotes $p < .001$ compared to LFS control mice ($n = 11$ and $n = 12$ mice per LFS and HFS diet groups, respectively).

Following the obesogenic diet, absolute GA muscle mass was significantly higher in obese mice ($t(21) = 3.139, p = .005$). However, when normalized to body mass, relative GA muscle mass was significantly lower ($t(21) = -10.114, p < .001$) in animals fed the HFS diet compared to their normal-weight counterparts (Table 4.1, figure 4.2). In contrast, absolute TA muscle mass was no different between the two experimental diet

groups ($t(21) = 1.124, p = .274$), but TA mass was significantly reduced in HFS-fed mice ($t(21) = -8.943, p < .001$) when expressed relative to body mass (Table 4.1, figure 4.3).

Table 4.1. Body mass, epididymal fat mass and muscle mass at study completion

| Outcome Variable | LFS-fed mice ($n = 11$) | HFS-fed mice ($n = 12$) | p -value |
|---|------------------------------|------------------------------|------------|
| Final total body mass (g) | 26.9 ± 1.1 | 41.5 ± 1.0 | .001* |
| Epididymal fat mass (g) | $.5 \pm .1$ | $2.3 \pm .2$ | .001† |
| Absolute GA muscle mass (mg) | 330.6 ± 4.0 | 351.7 ± 5.3 | .005‡ |
| Absolute TA muscle mass (mg) | 118.6 ± 3.5 | 123.9 ± 3.9 | .274‡ |
| GA muscle mass relative to body mass (mg/g) | $12.3 \pm .2$ | $8.6 \pm .3$ | .001‡ |
| TA muscle mass relative to body mass (mg/g) | $4.4 \pm .1$ | $3.0 \pm .1$ | .001‡ |

Note: Values are means \pm SEM. Muscle masses refer to combined mass from right and left legs, and absolute and relative GA mass refers to mixed muscle mass prior to red and white muscle separation. Asterixis pertain to statistical tests from which p -values were derived; * Mixed method (2x13) ANOVA and pairwise comparisons with Bonferroni adjustment, † Mann-Whitney-U test (one-tailed), ‡ Independent t-test (two-tailed). Sample size for all variables was $n = 11$ and $n = 12$ mice per LFS and HFS diet groups, respectively.

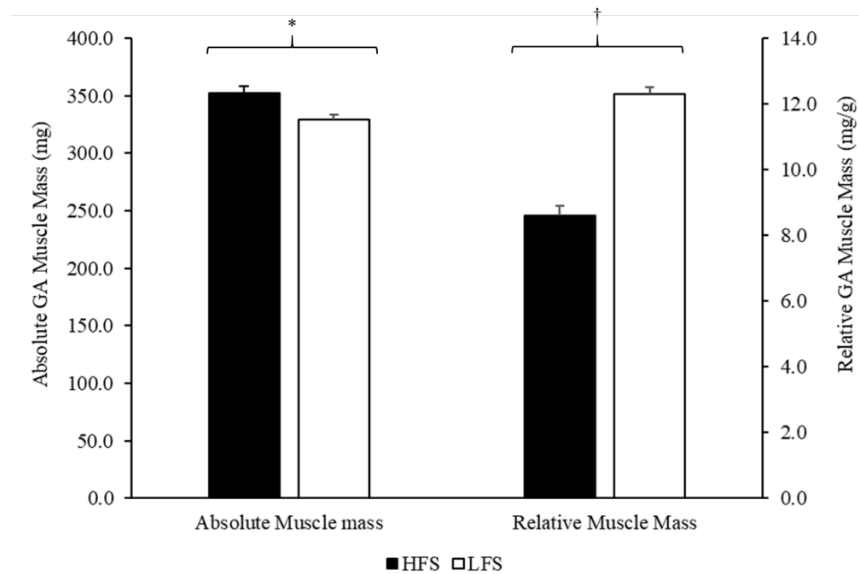


Figure 4.2. Change in GA muscle mass with DIO. Data are displayed as mean \pm SEM for each group with absolute muscle mass and muscle mass relative to body mass represented on the primary and secondary y-axes, respectively. Independent t-tests (two-tailed) revealed * absolute GA muscle mass was greater ($p = .005$), but † relative GA muscle mass was lower in mice with DIO ($p < .001$) ($n = 11$ and $n = 12$ mice per LFS and HFS diet groups, respectively).

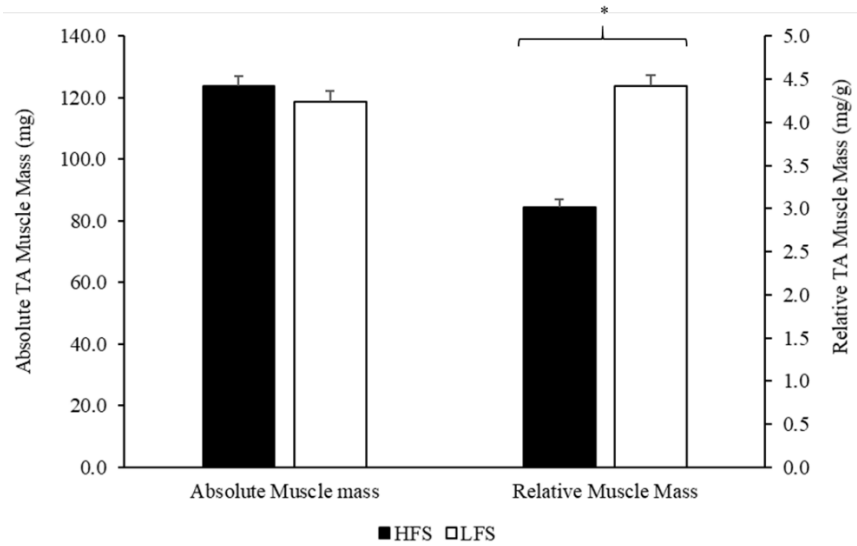


Figure 4.3. Change in TA muscle mass with DIO. Data are displayed as mean \pm SEM for each group with absolute muscle mass and muscle mass relative to body mass represented on the primary and secondary y-axes, respectively. Independent t-tests (two-tailed) revealed * absolute TA muscle mass was not different between diet groups ($p = .274$), however; † relative TA muscle mass was lower in mice with DIO ($p < .001$) ($n = 11$ and $n = 12$ mice per LFS and HFS diet groups, respectively).

Blood Glucose

A mixed method (2x4) ANOVA revealed a significant interaction effect between diet group assignment and change in blood glucose assessed during the feeding phase of the study ($F(3,63) = 20.14$, $p < .001$). Although Bonferroni post hoc tests showed no between-group difference in blood glucose at the onset of experimental feeding (HFS 206.8 ± 7.6 mg/dL vs LFS 199.4 ± 8.0 mg/dL, $F(1,21) = .46$, $p = .505$), blood glucose was significantly higher in mice fed the HFS diet ($F(1,21) = 34.65$, $p < .001$) by the second blood sampling time point (i.e., experimental week 5) (figure 4.4). The significant difference in blood glucose between HFS-fed mice and the LFS-fed controls persisted for all subsequent blood samples ($p < .001$ for all), despite an unexpected rise in blood

glucose noted in the LFS control mice at euthanasia (LFS week nine 158.9 ± 8.8 mg/dL vs LFS week thirteen 188.6 ± 8.1 mg/dL, $F(1,21) = 17.2$, $p = .001$) (figure 4.4).

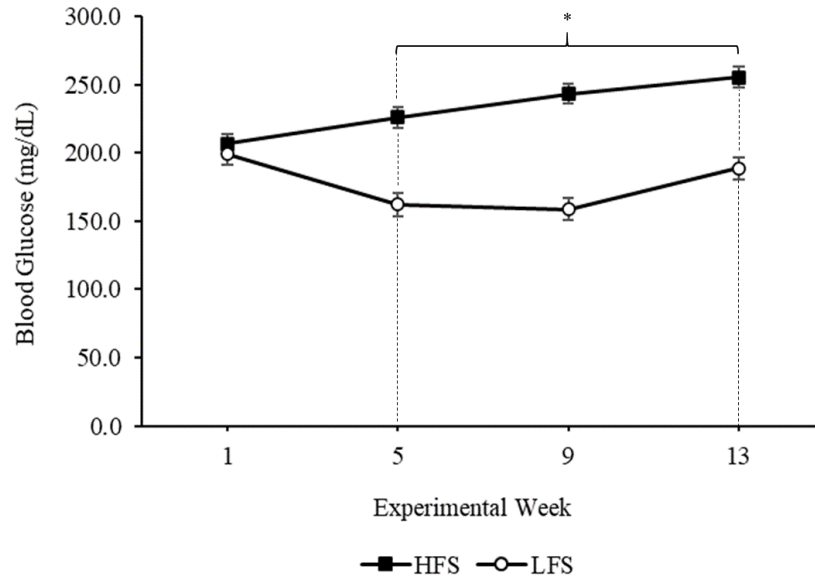


Figure 4.4. Change in blood glucose with high-fat, high-sucrose feeding. A mixed method (2x4) ANOVA and pairwise comparisons using Bonferroni adjustment were used to compare monthly change in blood glucose between LFS- and HFS-fed mice over the experimental feeding period. Data are displayed as mean \pm SEM at each time point and * denotes $p < .001$ compared to LFS control mice ($n = 11$ and $n = 12$ mice per LFS and HFS diet groups, respectively).

Muscle Strength

Strength was assessed during the penultimate week of experimental feeding via the forelimb weight lifting test. Absolute strength scores and strength scores adjusted to body mass (relative strength score) are displayed in figure 4.5. Independent t-tests revealed no difference in absolute forelimb strength between obese and LFS-control mice ($t(21) = -.33$, $p = .373$). However, when adjusted to body mass, relative forelimb strength score was significantly lower in HFS-fed mice when compared to their normal-weight counterparts ($t(21) = -2.07$, $p = .025$).

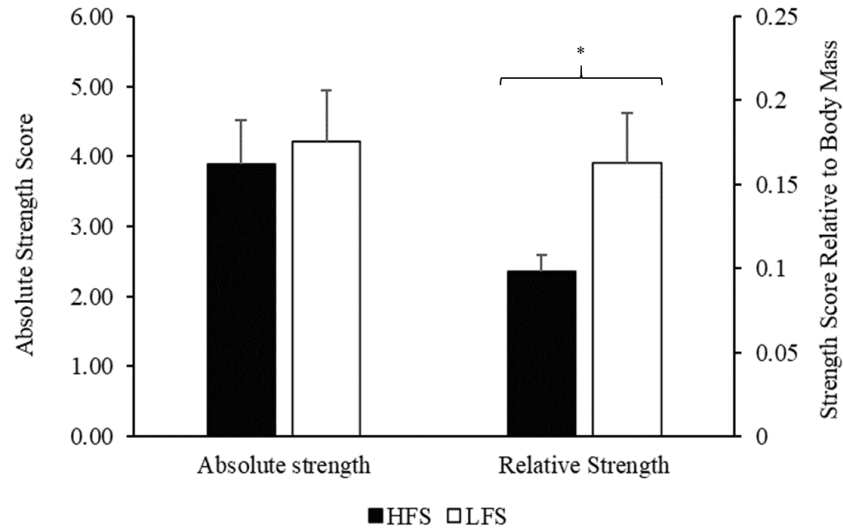


Figure 4.5. The impact of high-fat, high-sucrose feeding on forelimb strength. Independent t-tests were used to compare absolute strength scores (primary y-axis) and strength scores normalized to test-day body mass (secondary y-axis) between LFS- and HFS-fed mice toward the end of the experimental feeding period. Data are displayed as mean \pm SEM and * denotes $p = .025$ compared to LFS control mice ($n = 11$ and $n = 12$ mice per LFS and HFS diet groups, respectively).

Intramuscular Inflammation and Oxidative Stress

Gastrocnemius and TA muscle concentrations of the pro-inflammatory cytokines (IFN- γ and TNF- α) did not differ ($p > .050$) between obese and control mice (Table 4.2). However, oxidative stress (protein carbonyl concentration) was significantly elevated within the GA ($t(14) = 2.32, p = .036$) and TA ($t(21) = 2.28, p = .033$) muscles of mice with DIO (figure 4.6).

Table 4.2. A comparison of GA and TA muscle IFN- γ and TNF- α (ng/mg) protein concentrations between obese and normal-weight mice

| Pro-Inflammatory Cytokine | LFS-fed mice | HFS-fed mice | <i>t</i> -value | <i>df</i> | <i>p</i> -value |
|---------------------------|--------------------|-------------------|-----------------|-----------|-----------------|
| IFN- γ (GA muscle) | 1.29 \pm .02 | 1.31 \pm .07 | .264 | 14 | .796 |
| IFN- γ (TA muscle) | 1.81 \pm .06 | 1.94 \pm .05 | 1.831 | 21 | .081 |
| TNF- α (GA muscle) | 241.94 \pm 10.35 | 243.07 \pm 7.18 | .089 | 14 | .930 |
| TNF- α (TA muscle) | 214.40 \pm 4.46 | 231.32 \pm 7.20 | 1.954 | 21 | .064 |

Note: Values are means \pm SEM. Independent t-tests (two-tailed) were used to compare all variables between LFS- and HFS-fed mice ($n = 8$ GA samples per diet group, $n = 11$ and $n = 12$ TA samples in LFS and HFS diet groups, respectively).

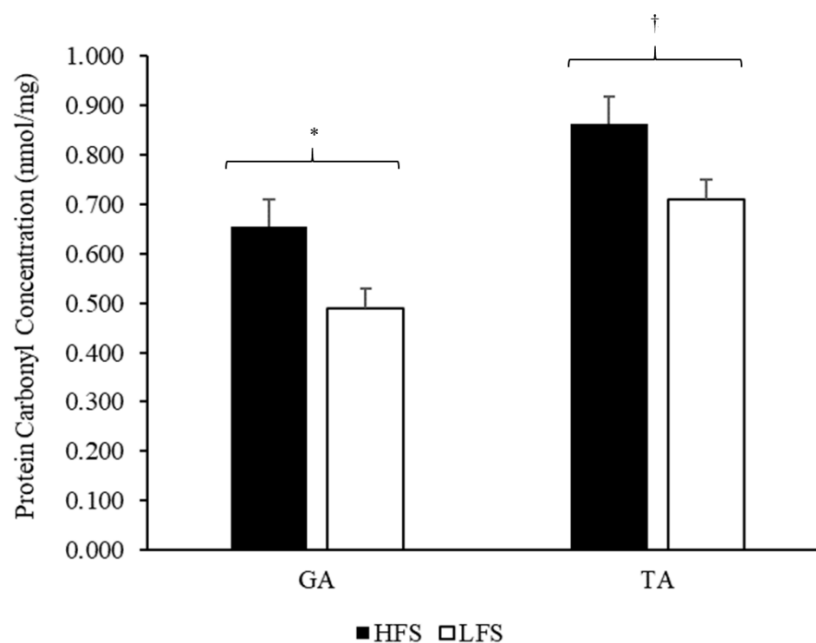


Figure 4.6. Change in GA and TA muscle protein carbonyl content in response to high-fat, high-sucrose feeding. Data are presented as mean \pm SEM and independent t-tests (two-tailed) were used to compare between group differences in protein carbonyl concentration in both GA and TA muscles. Asterix denote * ($p = .036$) and † ($p = .033$) compared to LFS-fed control mice ($n = 8$ GA samples per diet group; $n = 11$ and $n = 12$ TA samples in LFS and HFS diet groups, respectively).

Alterations in Intramuscular iProt Content

Total proteasome content (the α -7 subunit) was no different in the GA muscle (HFS $1.96 \pm .07$ ng/mg vs LFS $1.78 \pm .11$ ng/mg, $U = 20.50$, $p = .234$) or TA muscle (HFS $1.54 \pm .12$ ng/mg vs LFS $1.67 \pm .08$ ng/mg, $U = 93.00$, $p = .104$) of mice with or without DIO. When compared to mice fed the LFS diet, protein concentrations of the LMP7 subunit were significantly lower ($p = .020$) in the GA muscle of obese mice, however; the LMP2 and MECL-1 subunits were unaffected ($p > .050$) by HFS feeding (Table 4.3). In contrast, intramuscular MECL-1 concentrations were reduced ($p = .043$) in the TA muscle of the obese mice, whereas the content of the LMP7 and LMP2 subunits were unaltered ($p > .050$) by DIO (Table 4.3).

Table 4.3. A comparison of iProt catalytic subunit protein concentrations in the GA and TA muscle of mice with and without DIO

| iProt subunit | LFS-fed mice | HFS-fed mice | <i>t</i> -value | <i>df</i> | <i>p</i> -value |
|--------------------|----------------|-----------------|-----------------|-----------|-----------------|
| LMP2 (GA muscle) | $5.41 \pm .32$ | $4.75 \pm .37$ | -1.362 | 14 | .195 |
| LMP2 (TA muscle) | $9.95 \pm .70$ | $10.19 \pm .39$ | .318 | 21 | .753 |
| MECL-1 (GA muscle) | $2.50 \pm .15$ | $2.22 \pm .15$ | -1.357 | 14 | .196 |
| MECL-1 (TA muscle) | $2.48 \pm .07$ | $2.27 \pm .07$ | -2.153 | 21 | .043* |
| LMP7 (GA muscle) | $2.27 \pm .10$ | $1.92 \pm .09$ | -2.617 | 14 | .020* |
| LMP7 (TA muscle) | $2.12 \pm .06$ | $2.22 \pm .06$ | 1.225 | 21 | .234 |

Note: Values are means \pm SEM, and protein concentrations displayed are normalized to the total proteasome content (the α -7 subunit) contained within each muscle sample. Independent *t*-tests (two-tailed) were used to compare all variables between LFS- and HFS-fed mice ($n = 8$ GA samples per diet group, $n = 11$ and $n = 12$ TA samples in LFS and HFS diet groups, respectively). * denotes between-group significance at the $p < .05$ level of confidence.

Alterations in Intramuscular Proteasome Activity

When compared to normal-weight control mice, iProt-specific chymotrypsin-like activity was significantly lower in both the GA ($t(14) = -2.81$, $p = .014$) and TA ($t(14) = -2.46$, $p = .028$) muscles of mice with DIO (figure 4.7). Due to the large sample volumes

required for the assay, non-specific/total proteasome chymotrypsin-like activity was assessed in GA muscle samples only. Subsequent independent t-tests revealed total proteasome activity was also significantly reduced in the obese animals ($t(14) = -2.24, p = .042$) (figure 4.8).

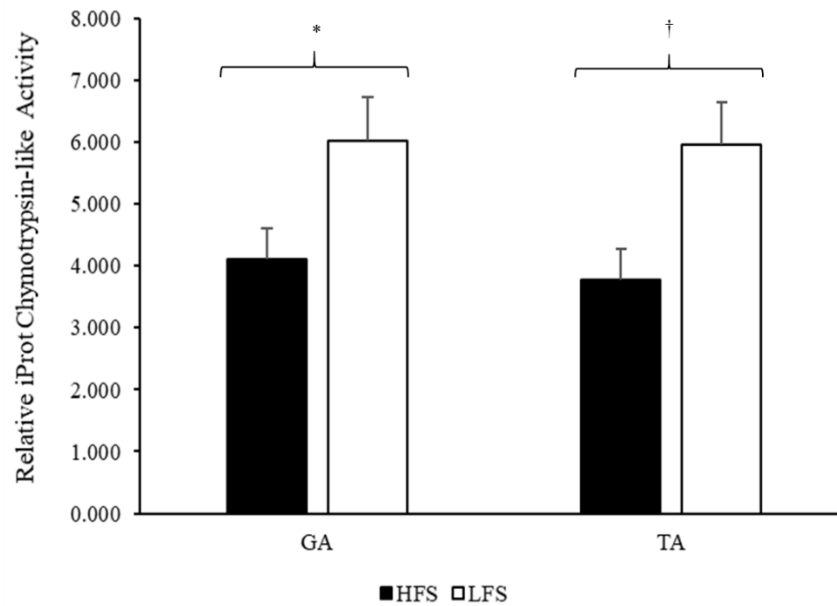


Figure 4.7. Change in GA and TA muscle iProt-specific chymotrypsin-like activity in response to a high-fat, high-sucrose diet. Data are mean (nmol/ng/min) \pm SEM for each group and presented as chymotrypsin-like activity normalized to the total proteasome content (i.e., the α -7 subunit) contained within each muscle sample. Independent t-tests (two-tailed) were used to compare between group differences in iProt catalytic activity in both GA and TA muscle groups ($n = 8$ muscle samples per diet group for all assays). Asterixis denote * ($p = .014$) and † ($p = .028$) compared to LFS-fed control mice.

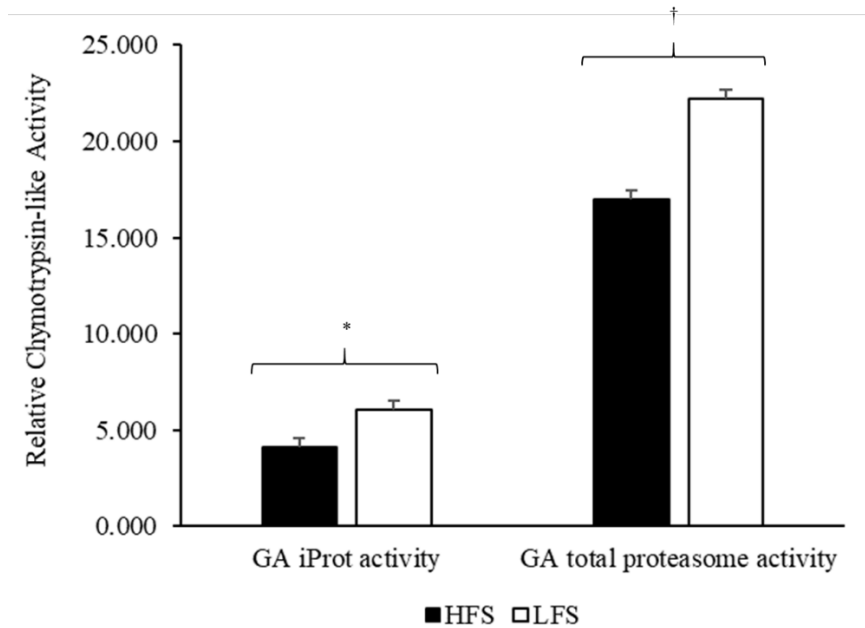


Figure 4.8. Comparison of iProt-specific and total proteasome chymotrypsin-like activity in the GA muscle of mice with and without DIO. Data are mean (nmol/ng/min) \pm SEM for each group and presented as chymotrypsin-like activity normalized to the total proteasome content contained within each muscle sample. Independent t-tests (two-tailed) were used to compare between group differences in catalytic activity ($n = 8$ muscle samples per diet group for all assays). Asterix denote * ($p = .014$) and † ($p = .042$) compared to LFS-fed control mice.

Discussion

The present study sought to elucidate whether a high-fat, high-sucrose diet alters intramuscular iProt subunit content and catalytic activity in wild-type (WT) mice to identify a possible mechanism for impaired muscle proteostasis thought to occur with obesity (15, 20, 27, 49). Our results show for the first time that although total proteasome content was unchanged by DIO, there were intrinsic differences in iProt β -subunit composition in the muscle of obese animals, and chymotrypsin-like activity was significantly reduced. Additionally, the decrease in iProt activity noted with HFS-feeding coincided with an intramuscular accumulation of oxidatively modified proteins (protein

carbonyls), as well as reductions in body mass-adjusted muscle mass and strength. In contrast, muscle inflammation (IFN- γ and TNF- α content) was unaffected by obesity.

A plethora of research indicates obesity-associated chronic overconsumption and the intramuscular deposition of surplus lipids creates an increasingly lipotoxic environment (15, 20, 27, 37, 49). Long-term exposure to such conditions places myocellular proteins at high risk of oxidative modification and damage, such as carbonylation (2, 15, 20, 27, 28, 37, 108, 109). Consequently, the increase in protein carbonyls noted within the GA and TA muscle of obese mice in the current study, was unsurprising. As protein oxidation is an irreversible post-translational loss-of-function modification (2, 27, 28, 108, 109), the removal of these damaged proteins is vital to preserve protein homeostasis and normal cell function (19, 110).

Skeletal muscle contains a network of protein quality control systems to regulate proteostasis. However, the proteasome system is responsible for eliminating oxidized proteins (24, 25, 29, 31, 147), and the iProt is considered more efficient in carrying out this function when compared to the standard proteasome variants (29, 36). The catalytic subunits of the iProt are also preferentially upregulated over those of the standard proteasome in situations of inflammation and/or oxidative stress (22, 23, 29, 31, 36, 37).

Considering obesity is a disease of chronic systemic inflammation and oxidative stress (1, 10, 88, 91, 96, 97, 107), one would assume the abovementioned stressors would stimulate a compensatory rise in iProt subunit content and activity to protect cells from damage. In support of the latter hypothesis, we previously showed 12-weeks of high-fat feeding (45% kcal fat) caused a commensurate increase in both oxidative stress (lipid peroxidation) and iProt content (the LMP7 subunit) in the GA muscle of WT mice,

despite no change to intramuscular inflammation. Insufficient tissue samples prevented the measurement of iProt enzymatic activity (49). While the current study found inflammation was similarly unchanged within obese muscle of WT mice, alterations to the iProt subunits were opposing. Specifically, a diet high in both fat and sucrose induced a significant reduction in the LMP7 and MECL-1 subunits within the GA and TA muscles, respectively. Immunoproteasome chymotrypsin-like activity was also reduced in both muscle groups of HFS-fed mice. As intramuscular inflammation was unaltered, and oxidative stress was elevated in both our studies, the cause for such discordant observations in the iProt may relate to other minor differences in experimental design.

For instance, recent evidence indicates when epithelial kidney cells were exposed to fatty acids (palmitate) for short durations *in vitro*, the iProt subunits were subsequently increased. However, prolonged exposure to palmitate reduced iProt subunit content (125). Although two-dimensional cell culture models cannot fully replicate the complex cell-macronutrient interactions within the natural *in vivo* environment (148), and the translatability to myocytes is unknown, the findings of Lee et al. (125), are consistent with the intramuscular iProt alterations noted in the present study. Given the experimental feeding duration was identical for our prior (49) and current work, it is possible dietary elevations in both fat and sucrose accelerates and/or has an additive effect on iProt dysregulation when compared to a diet high in fat alone. While further confirmation is warranted, these data suggest chronic macronutrient overload with obesity downregulates iProt subunit expression and catalytic activity in numerous cell types. Since the iProt is a prime mediator in the removal of oxidized proteins (29, 32),

such a reduction in iProt activity also provides a plausible explanation for the coincident increase in intramuscular carbonyls noted in the obese mice of the current investigation.

However, despite differences in efficacy (29, 32), a functional overlap between the iProt and standard 20S proteasome exists, which includes the degradation of oxidized proteins (24, 25, 29, 31, 35, 120). Although the β -subunit content of the standard proteasome was not specifically measured, the proteasome core complex is known to exhibit dynamic structural plasticity, and transforms based on cellular requirements (35, 120). Therefore, as total proteasome content was unchanged in the current study, but certain iProt β -subunits were reduced within obese muscle, a compensatory increase in the corresponding β -subunits of the standard proteasome likely occurred. Nevertheless, total proteasome chymotrypsin-like activity was reduced, which could not be fully accounted for by the reduction in iProt-specific activity alone. Consequently, intramuscular proteasome dysfunction with obesity may not be restricted to the iProt. Our observations suggest obesity may also have a detrimental effect on the standard proteasome and any associated compensatory attempts to contain oxidative protein damage as a result of reduced iProt activity. Further research is required to confirm the extent to which obesity alters the activity of the individual proteasome variants and their ability to maintain muscle proteostasis. In addition, the precise underlying mechanisms driving such proteasome dysregulation in the obese state remains unclear.

Nevertheless, oxidized proteins have a propensity to aggregate in situations of chronic oxidative stress (31, 35, 37). While previous investigations in cellular aging show these protein aggregates can still bind to the outer α -subunits of the 20S proteasome, they are often too large to enter the catalytic core (50–52). Consequently, further protein

aggregation occurs, which may ultimately result in proteasome sequestration-induced inhibition (27, 50, 51, 53). Alternatively, similar studies indicate the outer proteasome subunits are also susceptible to oxidative modification under conditions of heightened oxidative stress (19, 27, 149). Moreover, an increase in oxidized proteasome adducts was previously shown to correlate with reduced catalytic activity (149). Considering the outer α -subunit structure is identical among all the different proteasome variants (23, 31, 35), such post-translational loss-of-function modifications and/or sequestration by large protein aggregates could account for the decrease in iProt and total proteasome activity noted in obese animals in our study.

Regardless of the underlying cause, compromised proteasome function coupled with the intramuscular accumulation of oxidatively damaged proteins with obesity is noteworthy. As impaired proteostasis diminishes muscle integrity (2, 19, 110), the inability to contain oxidative protein modification and damage, via the iProt and standard 20S proteasome, may predispose obese individuals to reductions in muscle mass and strength. Indeed, relative forelimb strength was significantly reduced in the obese mice of the current study. Although absolute muscle mass was unaltered (TA) or increased (GA) with DIO, when normalized to total body mass, both TA and GA muscle mass were significantly lower in HFS-fed mice. The discrepant response in TA and GA absolute mass to HFS feeding was unsurprising. For instance, the GA muscle is a primary weight-bearing muscle of the hindlimb and subjected to a constant overloading effect from the elevated body mass of obesity (18, 71). In contrast, the TA muscle is non-weight bearing, and thus, not exposed to the same body mass-induced muscle “training” effect (71). Therefore, the increase in absolute GA muscle mass suggests weight-bearing muscle

groups are somewhat protected from obese sarcopenia when compared to non-weight bearing muscle groups. However, the reduction in relative muscle mass also suggests the GA may be in the early stages of muscle atrophy. As reduced relative muscle mass in both the TA and GA coincided with the accumulation of oxidized proteins, there is reason to believe the change in muscle mass could be linked to impaired proteostasis, conceivably via proteasome dysfunction. Additionally, as skeletal muscle is responsible for 85% of glucose disposal (150), such a decline in muscle mass may explain why obese mice displayed signs of hyperglycemia. Consequently, the development of insulin resistance and type II diabetes in obese individuals could, at least partially, be explained by a diminished proteasome-mediated regulation of muscle proteostasis and mass.

Although the current study is the first to perform such a comprehensive assessment of iProt content in conjunction with measures of iProt-specific and non-specific proteasome activity in obese muscle, this research is not without limitations. First, the use of male mice limits the generalizability of our findings. As the metabolic derangements in response to HFS-feeding is blunted in female mice, males, particularly of the C57BL/6J strain, are currently considered better models of human obesity (63–65). Second, all muscle analyses were restricted to type II fiber-predominant muscle groups (69, 70), and whether similar alterations occur in type I muscle groups with obesity, is unknown. Considering fast-twitch muscle is more susceptible to lipid accumulation and related stress (67, 68), we felt the selection of these particular muscle groups were appropriate given the aims of the current study. In addition, owing to limited tissue homogenate volumes, comparative measures between the iProt and standard proteasome subunits contained within muscle were not assessed. Therefore, we cannot confirm

whether reductions in the iProt β -subunits induced a compensatory increase in the corresponding standard proteasome subunits. However, as total proteasome content was unchanged in obese muscle, such a compensatory increase in the standard proteasome, is plausible. Similarly, although we clearly show HFS feeding caused a significant reduction in iProt and total proteasome chymotrypsin-like activity, we did not include a measure of standard proteasome-specific activity. Nevertheless, prior research suggests conditions of inflammation and oxidative stress promote iProt expression and activity at the expense of the standard proteasomes in an attempt to regain cellular protein homeostasis (29, 32). Consequently, as obesity is a disease of chronic systemic inflammation and oxidative stress (1, 10, 88, 91, 96, 97, 107), and since intramuscular alterations to iProt activity with obesity were previously unknown, the primary aim of the current study was to evaluate iProt activity. Further research is required to clarify whether the proteasome variants are impacted differentially by obesity and the key upstream mechanisms involved in mediating dysfunction. Lastly, limited tissue samples also restricted the analysis of iProt activity to chymotrypsin-like activity. However, chymotrypsin-like activity is considered the rate-limiting step in proteolysis (151) and vital for the breakdown of oxidized proteins (36). Since the iProt displays enhanced chymotrypsin-like activity when compared to the standard proteasome (22, 35, 36), we felt a comprehensive assessment of all the iProt proteases was unnecessary.

Conclusions

Effective maintenance of muscle mass is a highly regulated, complex process dependent on a tight balance between muscle protein synthesis and breakdown (1–7). As numerous exogenous and endogenous stressors are known to accumulate in obese

muscle, sustaining protein homeostasis is inherently challenging (1, 8, 12, 90, 93–95). Indeed, the current investigation demonstrates oxidatively damaged proteins were increased in the muscle of obese mice, which coincided with a reduction in both iProt and total proteasome activity. The inability to contain such a disruption to intramuscular proteostasis, conceivably via the proteasome, could be a key determining event in the loss of muscle mass and function thought to occur with obesity (1, 8–18). Considering the loss of muscle mass and strength amplify the risk of morbidity and mortality (13, 18, 54–58), there is much merit for future research to further delineate the specific upstream mediators of obesity-associated proteasome dysregulation and the ability to maintain muscle proteostasis. Although the iProt is regarded as the more effective proteasome variant in the removal of oxidized proteins (29, 32, 35, 36), confirming the extent to which each individual proteasome contributes to impaired muscle proteostasis in the obese state would provide significant therapeutic opportunities. For instance, the ability to manipulate the specific proteasome sub-type with the greatest impact on obese muscle proteostasis could provide a novel mechanism to optimize the maintenance of muscle mass and function in obesity.

CHAPTER FIVE

Conclusions

The effective maintenance of muscle mass is a highly regulated, complex process dependent on a tight balance between muscle protein synthesis and breakdown (1–7). Research over the last five decades highlights the critical role of the standard proteasome in sustaining protein homeostasis, and how aberrations in this proteolytic system are linked to numerous diseases, including muscle atrophy (19, 25, 111, 126–128). Nevertheless, more recent evidence suggests immunoproteasome (iProt) dysregulation may also be an important intermediary in muscle pathology (41, 46, 49, 120, 129–131). Consequently, the ability to quantify the proteolytic activity of the different proteasome isoforms is crucial to further research in numerous atrophic disorders.

The classical and most commonly cited method for determining proteasome activity *in vitro* is through the use of fluorescently tagged peptide substrates specific for the catalytic enzymes of the proteasome (73, 132, 133). During the assay, the sample of interest is incubated with these fluoropeptide substrates (62, 132, 133) in the presence and absence of a proteasome inhibitor. The use of an inhibitor (i.e., negative control) is vital to ensure the enzymatic activity measured can be ascribed to the proteasome, and not to other proteolytic enzymes contained within the sample (33, 61, 62, 73, 74, 76). Although several fluorometric assay kits for measuring the enzymatic activity of the standard proteasome are commercially available (41), few are specific to the iProt. Moreover, the assays deemed applicable to the iProt, were validated on mouse splenic

samples (60), and not skeletal muscle. As the iProt content of the spleen is comparatively greater than other non-lymphoid organs (61, 73), the recommended assay conditions and inhibitor concentrations may not translate to other tissues such as skeletal muscle (62). Consequently, the study described in Chapter Three sought to conduct preliminary trials to optimize the assay procedures listed by the manufacturer in murine skeletal muscle. Two specific aims were assessed.

The purpose of the initial trial was to use the proprietary assay kit to test a range of muscle protein concentrations (1 mg, 3 mg and 5 mg protein) to determine the minimal protein content that would yield sufficient fluorescence signal intensity (i.e., signal within the mid-range of the standard curve) during the assay. Unsurprisingly, our results show fluorescence intensity is significantly improved in samples with higher protein concentrations. Nevertheless, we also demonstrate concentrations as low as 3 mg protein will still yield sufficient signal to enable the further calculation of proteasome activity (by extrapolation to the standard curve) (62). The results from this trial provided much needed guidance for future analyses within the current study, as well as those of Chapter Four. Indeed, given that mouse muscle sample volumes are typically limited, and owing to the large sample volume requirements of the assay, establishing the minimal concentrations required to gain optimal results, whilst also preserving limited sample, is vital.

Consequently, muscle homogenate containing 3 mg protein was utilized for the second phase of investigations performed in Chapter Three. Specifically, we performed dose-response trials on murine muscle homogenate using two different proteasome inhibitors; an iProt-specific (ONX-0914) inhibitor, as well as MG-132, known to inhibit

all proteasome isoforms. The overall goal of the dose-response trials was to test whether manufacturer- and surrounding literature-recommended dosages visibly lowered proteasome activity in skeletal muscle homogenate. The observations made from these trials, together with manufacturer recommendations and inferences from the surrounding literature, allowed us to make informed decisions regarding appropriate inhibitor doses to use with skeletal muscle samples in the analyses of Chapter Four, as well as any research conducted in the future. Specifically, the study depicted in Chapter Four sought to apply the knowledge gained regarding the analysis of iProt and total proteasome activity in normal, healthy murine skeletal muscle, and extend the investigations to muscle tissue from mice with diet-induced obesity.

Numerous exogenous (e.g., dietary fat) and endogenous (e.g., oxidative free radicals) stressors are known to accumulate in obese muscle (1, 8, 12, 90, 93–95). Consequently, sustaining intramuscular protein homeostasis (proteostasis) is inherently challenging (1, 8, 12, 90, 93–95) and may predispose obese individuals to reductions in muscle mass and/or function (12, 15, 17–20, 59). Indeed, the investigation of Chapter Four demonstrates oxidatively damaged proteins accumulated in the muscle of obese mice. Notably, these alterations within muscle also coincided with reduced iProt and total proteasome activity, as well as a decrease in relative muscle mass and strength. Since the proteasome, particularly the iProt, is a prime mediator in the removal of oxidized proteins (29, 32), our findings suggest proteasome dysfunction could be a key determining event in the loss of intramuscular proteostasis with obesity. As impaired proteostasis diminishes muscle integrity (2, 19, 110), the inability to contain oxidative protein damage via the proteasome, provides a plausible explanation for the loss of muscle mass and strength

observed in the obese mice described in Chapter Four. Considering muscle atrophy and reductions in strength amplify the risk of morbidity and mortality (13, 18, 54–58), future research is vital to delineate whether deficits in proteasome function noted in young obese individuals augment the loss of muscle already known to occur with age (152, 153).

There is also much merit for future work to determine the specific impact obesity has on the different proteasome variants, including standard-iProt hybrids, and their ability to maintain muscle proteostasis. Elucidating the extent to which each individual proteasome and/or proteasome hybrid contributes to impaired muscle proteostasis in the obese state would provide significant therapeutic opportunities. For instance, the ability to manipulate the specific proteasome sub-type with the greatest impact on obese muscle proteostasis could provide a novel mechanism to optimize the maintenance of muscle mass and thus function in obesity.

Moreover, determining whether decrements in intramuscular proteolytic function can be slowed and/or reversed via non-pharmacologic interventions such as exercise could be equally important for optimal muscle health and future health status.

Interestingly, a prior study conducted in our lab showed that intramuscular lipotoxicity was significantly reduced in obese mice 5 d following an acute bout of downhill running. Lipotoxicity in the muscle of high fat-fed mice was also reduced to levels consistent with their normal weight counterparts, and coincided with increased muscle concentrations of both the LMP7 and MECL-1 iProt subunits (49). As iProt function was not assessed, confirmatory research is warranted. Nevertheless, our prior work suggests a single bout of downhill treadmill running may yield protective effects in obese individuals by

reducing muscle oxidative stress via an upregulation of the iProt. Since the metabolic and cardiovascular demands of eccentric exercise are lower when compared to concentric exercise, this form of training is thought to promote better adherence rates in obese populations (154–156). Future investigations should thus ascertain whether eccentric exercise training is also superior in mediating the intramuscular proteasome response to obesity. Results from such studies would provide much needed insight for the determination of optimal exercise interventions for the management of obesity.

However, skeletal muscle contains several quality control systems that regulate protein homeostasis (25, 28, 48, 111, 116), and the potential interaction between the proteasome and other proteolytic mechanisms cannot be ignored (25, 28, 157). For example, Xie et al. (157) recently showed the LMP7 subunit of the iProt downregulates the autophagy gene, ATG5, and thus the autophagy-lysosomal pathway in cardiomyocytes. Furthermore, the LMP7-mediated reduction in autophagy promoted an increase in cardiomyocyte size. Whether the iProt performs a similar function in skeletal muscle, and whether obesity upregulates intramuscular autophagy through impaired iProt activity, is unknown. Determining such potential coordinated actions between the major protein quality control systems in skeletal muscle, and the impact obesity may have on such interactions is also imperative to advance the development of therapeutics which enhance muscle mass maintenance.

Lastly, regulators of muscle mass may not be confined to the local muscle environment, but likely impacted by signals originating from other organs or tissues (12, 88, 158, 159). In particular, obesity-related fat accumulation within both visceral adipose tissue (VAT) and the liver is associated with reductions in muscle mass (12). The precise

way in which dysfunction within these organs alter muscle mass is currently unclear. However, as preliminary investigations suggest oxidative stress is shared among the obesity-induced pathologies of muscle, liver and VAT (12, 88, 158, 159), a subsequent multi-systemic dysregulation of proteolytic function is conceivable. Consequently, future research should also consider the potential signaling cross-talk between muscle and other organs and elucidate whether a central moderator of oxidative stress exists. Gaining an understanding of such molecular drivers of oxidative stress and impaired proteostasis would not only aid the treatment of obese muscle pathology, but could reveal a therapeutic avenue for treating a myriad of chronic diseases associated with obesity.

REFERENCES

1. Lynch GM, Murphy CH, Castro E de M, Roche HM. Inflammation and metabolism: the role of adiposity in sarcopenic obesity. *Proc Nutr Soc.* 2020;1–13.
2. Hipp MS, Kasturi P, Hartl FU. The proteostasis network and its decline in ageing. *Nat Rev Mol Cell Biol.* 2019;20(7):421–35.
3. Lecker SH, Solomon V, Mitch WE, Goldberg AL. Muscle Protein Breakdown and the Critical Role of the Ubiquitin-Proteasome Pathway in Normal and Disease States. *J Nutr.* 1999;129(1):227S-237S.
4. Beals JW, Burd NA, Moore DR, van Vliet S. Obesity Alters the Muscle Protein Synthetic Response to Nutrition and Exercise. *Front Nutr.* 2019;6:87.
5. Atherton PJ, Smith K. Muscle protein synthesis in response to nutrition and exercise. *J Physiol.* 2012;590(Pt 5):1049–57.
6. Kim I-Y, Deutz NEP, Wolfe RR. Update on maximal anabolic response to dietary protein. *Clin Nutr.* 2018;37(2):411–8.
7. Wolfe RR. Branched-chain amino acids and muscle protein synthesis in humans: myth or reality? *J Int Soc Sports Nutr.* 2017;14(1):30.
8. Barazzoni R, Bischoff SC, Boirie Y, et al. Sarcopenic obesity: Time to meet the challenge. *Clin Nutr Edinb Scotl.* 2018;37(6 Pt A):1787–93.
9. Brown LA, Lee DE, Patton JF, et al. Diet-induced obesity alters anabolic signalling in mice at the onset of skeletal muscle regeneration. *Acta Physiol.* 2015;215(1):46–57.
10. Collins KH, Herzog W, MacDonald GZ, et al. Obesity, Metabolic Syndrome, and Musculoskeletal Disease: Common Inflammatory Pathways Suggest a Central Role for Loss of Muscle Integrity. *Front Physiol.* 2018;9:112.
11. D’Souza DM, Trajcevski KE, Al-Sajee D, et al. Diet-induced obesity impairs muscle satellite cell activation and muscle repair through alterations in hepatocyte growth factor signaling. *Physiol Rep.* 2015;3(8):e12506.
12. Sinha I, Sakthivel D, Varon DE. Systemic Regulators of Skeletal Muscle Regeneration in Obesity. *Front Endocrinol* [Internet]. 2017 [cited 2018 Oct 20];8 Available from: <https://www.ncbi.nlm.nih.gov/pmc/articles/PMC5311070/>. doi:10.3389/fendo.2017.00029.
13. Tomlinson DJ, Erskine RM, Morse CI, Winwood K, Onambélé-Pearson G. The impact of obesity on skeletal muscle strength and structure through adolescence to old age. *Biogerontology.* 2016;17:467–83.

14. Espinosa A, Henríquez-Olguín C, Jaimovich E. Reactive oxygen species and calcium signals in skeletal muscle: A crosstalk involved in both normal signaling and disease. *Cell Calcium*. 2016;60(3):172–9.
15. Capel F, Pinel A, Walrand S. Accumulation of intramuscular toxic lipids, a link between fat mass accumulation and sarcopenia. *OCL*. 2019;26:24.
16. Abrigo J, Rivera JC, Aravena J, et al. High Fat Diet-Induced Skeletal Muscle Wasting Is Decreased by Mesenchymal Stem Cells Administration: Implications on Oxidative Stress, Ubiquitin Proteasome Pathway Activation, and Myonuclear Apoptosis. *Oxid Med Cell Longev*. 2016;2016:1–13.
17. Valenzuela PL, Maffiuletti NA, Tringali G, De Col A, Sartorio A. Obesity-associated poor muscle quality: prevalence and association with age, sex, and body mass index. *BMC Musculoskelet Disord*. 2020;21(1):200.
18. Tallis J, James RS, Seebacher F. The effects of obesity on skeletal muscle contractile function. *J Exp Biol*. 2018;221(13):jeb163840.
19. Jaisson S, Gillery P. Impaired proteostasis: role in the pathogenesis of diabetes mellitus. *Diabetologia*. 2014;57(8):1517–27.
20. Bartelt A, Widenmaier SB. Proteostasis in thermogenesis and obesity. *Biol Chem*. 2020;401(9):1019–30.
21. Basler M, Claus M, Klawitter M, Goebel H, Groettrup M. Immunoproteasome Inhibition Selectively Kills Human CD14⁺ Monocytes and as a Result Dampens IL-23 Secretion. *J Immunol*. 2019;203(7):1776–85.
22. Angeles A, Fung G, Luo H. Immune and non-immune functions of the immunoproteasome. *Front Biosci Landmark Ed*. 2012;17:1904–16.
23. Raynes R, Pomatto LCD, Davies KJA. Degradation of oxidized proteins by the proteasome: Distinguishing between the 20S, 26S, and immunoproteasome proteolytic pathways. *Mol Aspects Med*. 2016;50:41–55.
24. Dikic I. Proteasomal and Autophagic Degradation Systems. *Annu Rev Biochem*. 2017;86(1):193–224.
25. Kitajima Y, Yoshioka K, Suzuki N. The ubiquitin–proteasome system in regulation of the skeletal muscle homeostasis and atrophy: from basic science to disorders. *J Physiol Sci*. 2020;70(1):40.
26. Lasker K, Forster F, Bohn S, et al. Molecular architecture of the 26S proteasome holocomplex determined by an integrative approach. *Proc Natl Acad Sci*. 2012;109(5):1380–7.
27. Hauck AK, Bernlohr DA. Oxidative stress and lipotoxicity. *J Lipid Res*. 2016;57(11):1976–86.

28. Reichmann D, Voth W, Jakob U. Maintaining a Healthy Proteome during Oxidative Stress. *Mol Cell*. 2018;69(2):203–13.
29. Pickering AM, Koop AL, Teoh CY, Ermak G, Grune T, Davies KJA. The immunoproteasome, the 20S proteasome and the PA28 $\alpha\beta$ proteasome regulator are oxidative-stress-adaptive proteolytic complexes. *Biochem J*. 2010;432(3):585–95.
30. Basler M, Kirk CJ, Groettrup M. The immunoproteasome in antigen processing and other immunological functions. *Curr Opin Immunol*. 2013;25(1):74–80.
31. Johnston-Carey HK, Pomatto LCD, Davies KJA. The Immunoproteasome in oxidative stress, aging, and disease. *Crit Rev Biochem Mol Biol*. 2016;51(4):268–81.
32. Pickering AM, Davies KJA. Degradation of damaged proteins: the main function of the 20S proteasome. *Prog Mol Biol Transl Sci*. 2012;109:227–48.
33. Dahlmann B. Role of proteasomes in disease. *BMC Biochem*. 2007;8(Suppl 1):S3.
34. Muchamuel T, Basler M, Aujay MA, et al. A selective inhibitor of the immunoproteasome subunit LMP7 blocks cytokine production and attenuates progression of experimental arthritis. *Nat Med*. 2009;15(7):781–7.
35. Ferrington DA, Gregerson DS. Immunoproteasomes: structure, function, and antigen presentation. *Prog Mol Biol Transl Sci*. 2012;109:75–112.
36. Abi Habib J, De Plaen E, Stroobant V, et al. Efficiency of the four proteasome subtypes to degrade ubiquitinated or oxidized proteins. *Sci Rep*. 2020;10(1):15765.
37. Jung T, Höhn A, Grune T. The proteasome and the degradation of oxidized proteins: Part II – protein oxidation and proteasomal degradation. *Redox Biol*. 2014;2:99–104.
38. Seifert U, Bialy LP, Ebstein F, et al. Immunoproteasomes Preserve Protein Homeostasis upon Interferon-Induced Oxidative Stress. *Cell*. 2010;142(4):613–24.
39. Nathan JA, Spinnenhirn V, Schmidtke G, Basler M, Groettrup M, Goldberg AL. Immuno- and constitutive proteasomes do not differ in their abilities to degrade ubiquitinated proteins. *Cell*. 2013;152(5):1184–94.
40. Kimura H, Caturegli P, Takahashi M, Suzuki K. New Insights into the Function of the Immunoproteasome in Immune and Nonimmune Cells. *J Immunol Res*. 2015;2015:541984.
41. Cui Z, Hwang SM, Gomes AV. Identification of the immunoproteasome as a novel regulator of skeletal muscle differentiation. *Mol Cell Biol*. 2014;34(1):96–109.
42. Ferrington DA, Husom AD, Thompson LV. Altered proteasome structure, function, and oxidation in aged muscle. *FASEB J Off Publ Fed Am Soc Exp Biol*. 2005;19(6):644–6.

43. Husom AD, Peters EA, Kolling EA, Fugere NA, Thompson LV, Ferrington DA. Altered proteasome function and subunit composition in aged muscle. *Arch Biochem Biophys*. 2004;421(1):67–76.
44. Chen C-NJ, Graber TG, Bratten WM, Ferrington DA, Thompson LV. Immunoproteasome in animal models of Duchenne muscular dystrophy. *J Muscle Res Cell Motil*. 2014;35(2):191–201.
45. Farini A, Sitzia C, Cassani B, et al. Therapeutic Potential of Immunoproteasome Inhibition in Duchenne Muscular Dystrophy. *Mol Ther J Am Soc Gene Ther*. 2016;24(11):1898–912.
46. Liu HM, Ferrington DA, Baumann CW, Thompson LV. Denervation-Induced Activation of the Standard Proteasome and Immunoproteasome. *PLoS One*. 2016;11(11):e0166831.
47. Bhattarai S, Ghannam K, Krause S, et al. The immunoproteasomes are key to regulate myokines and MHC class I expression in idiopathic inflammatory myopathies. *J Autoimmun*. 2016;75:118–29.
48. Lee DH, Goldberg AL. Proteasome inhibitors: valuable new tools for cell biologists. *Trends Cell Biol*. 1998;8(10):397–403.
49. Fletcher E, Gordon PM. Obesity-induced alterations to the immunoproteasome: a potential link to intramuscular lipotoxicity. *Appl Physiol Nutr Metab*. 2020;apnm-2020-0655.
50. Stenoien DL, Cummings CJ, Adams HP, et al. Polyglutamine-Expanded Androgen Receptors Form Aggregates That Sequester Heat Shock Proteins, Proteasome Components and SRC-1, and Are Suppressed by the HDJ-2 Chaperone. *Hum Mol Genet*. 1999;8(5):731–41.
51. Verhoef LGGC. Aggregate formation inhibits proteasomal degradation of polyglutamine proteins. *Hum Mol Genet*. 2002;11(22):2689–700.
52. Leeuwenburgh C, Rasmussen JE, Hsu FF, Mueller DM, Pennathur S, Heinecke JW. Mass spectrometric quantification of markers for protein oxidation by tyrosyl radical, copper, and hydroxyl radical in low density lipoprotein isolated from human atherosclerotic plaques. *J Biol Chem*. 1997;272(6):3520–6.
53. Shringarpure R, Davies KJA. Protein turnover by the proteasome in aging and disease. *Free Radic Biol Med*. 2002;32(11):1084–9.
54. Addison O, Marcus RL, Lastayo PC, Ryan AS. Intermuscular fat: a review of the consequences and causes. *Int J Endocrinol*. 2014;2014:309570.
55. Alley DE, Chang VW. The changing relationship of obesity and disability, 1988-2004. *JAMA*. 2007;298(17):2020–7.
56. Goodpaster BH, Thaete FL, Kelley DE. Thigh adipose tissue distribution is associated with insulin resistance in obesity and in type 2 diabetes mellitus. *Am J Clin Nutr*. 2000;71(4):885–92.

57. Ruiz JR, Sui X, Lobelo F, et al. Association between muscular strength and mortality in men: prospective cohort study. *BMJ*. 2008;337:a439.
58. Stenholm S, Mehta NK, Elo IT, Heliövaara M, Koskinen S, Aromaa A. Obesity and muscle strength as long-term determinants of all-cause mortality--a 33-year follow-up of the Mini-Finland Health Examination Survey. *Int J Obes* 2005. 2014;38(8):1126–32.
59. McGregor RA, Cameron-Smith D, Poppitt SD. It is not just muscle mass: a review of muscle quality, composition and metabolism during ageing as determinants of muscle function and mobility in later life. *Longev Heal*. 2014;3(1):9.
60. Ubiquitin-Proteasome Biotechnologies. Immunoproteasome Activity Fluorometric Assay Kit I - Protocol. 2012; [cited 2021 May 11] Available from: <https://www.ubpbio.com/index.php/product/kits/immunoproteasome-activity-fluorometric-assay-kit-i.html>.
61. Hussong SA, Kapphahn RJ, Phillips SL, Maldonado M, Ferrington DA. Immunoproteasome deficiency alters retinal proteasome's response to stress. *J Neurochem*. 2010;113(6):1481–90.
62. Kisselev AF, Goldberg AL. Monitoring Activity and Inhibition of 26S Proteasomes with Fluorogenic Peptide Substrates. *Methods in Enzymology*. Elsevier; 2005. p. 364–78. [cited 2021 May 12] Available from: <https://linkinghub.elsevier.com/retrieve/pii/S0076687905980300>.
63. Wang C-Y, Liao JK. A Mouse Model of Diet-Induced Obesity and Insulin Resistance. *Methods Mol Biol Clifton NJ*. 2012;821:421–33.
64. Williams LM, Campbell FM, Drew JE, et al. The Development of Diet-Induced Obesity and Glucose Intolerance in C57Bl/6 Mice on a High-Fat Diet Consists of Distinct Phases. *PLOS ONE*. 2014;9(8):e106159.
65. Della Vedova MC, Muñoz MD, Santillan LD, et al. A Mouse Model of Diet-Induced Obesity Resembling Most Features of Human Metabolic Syndrome. *Nutr Metab Insights*. 2016;9:NMI.S32907.
66. Kleinert M, Clemmensen C, Hofmann SM, et al. Animal models of obesity and diabetes mellitus. *Nat Rev Endocrinol*. 2018;14(3):140–62.
67. Hua N, Takahashi H, Yee GM, et al. Influence of muscle fiber type composition on early fat accumulation under high-fat diet challenge. *PloS One*. 2017;12(8):e0182430.
68. Duan Y, Li F, Tan B, Yao K, Yin Y. Metabolic control of myofibers: promising therapeutic target for obesity and type 2 diabetes: Myofibers and obesity. *Obes Rev*. 2017;18(6):647–59.
69. Augusto V, Padovani CR, Rocha Campos GE. Skeletal muscle fiber types in C57BL6J mice. *J Morphol Sci*. 2004;21(2):89–94.

70. Kammoun M, Cassar-Malek I, Meunier B, Picard B. A simplified immunohistochemical classification of skeletal muscle fibres in mouse. *Eur J Histochem EJH*. 2014;58(2):2254.
71. Rader EP, Faulkner JA. Recovery from contraction-induced injury is impaired in weight-bearing muscles of old male mice. *J Appl Physiol*. 2006;100(2):656–61.
72. Goldberg AL. Probing the Proteasome. *Trends Cell Biol*. 2016;26(11):792–4.
73. Liggett A, Crawford LJ, Walker B, Morris TCM, Irvine AE. Methods for measuring proteasome activity: Current limitations and future developments. *Leuk Res*. 2010;34(11):1403–9.
74. Rodgers KJ, Dean RT. Assessment of proteasome activity in cell lysates and tissue homogenates using peptide substrates. *Int J Biochem Cell Biol*. 2003;35(5):716–27.
75. Tsubuki S, Saito Y, Tomioka M, Ito H, Kawashima S. Differential Inhibition of Calpain and Proteasome Activities by Peptidyl Aldehydes of Di-Leucine and Tri-Leucine. *J Biochem (Tokyo)*. 1996;119(3):572–6.
76. Kisselev AF, Goldberg AL. Proteasome inhibitors: from research tools to drug candidates. *Chem Biol*. 2001;8(8):739–58.
77. Grune T. Oxidized protein aggregates: Formation and biological effects. *Free Radic Biol Med*. 2020;150:120–4.
78. Weber D, Davies MJ, Grune T. Determination of protein carbonyls in plasma, cell extracts, tissue homogenates, isolated proteins: Focus on sample preparation and derivatization conditions. *Redox Biol*. 2015;5:367–80.
79. Li R, Xia J, Zhang XI, et al. Associations of Muscle Mass and Strength with All-Cause Mortality among US Older Adults. *Med Sci Sports Exerc*. 2018;50(3):458–67.
80. Leong DP, Teo KK, Rangarajan S, et al. Prognostic value of grip strength: findings from the Prospective Urban Rural Epidemiology (PURE) study. *The Lancet*. 2015;386(9990):266–73.
81. Contet C. A comparison of 129S2/SvHsd and C57BL/6JOLA Hsd mice on a test battery assessing sensorimotor, affective and cognitive behaviours: implications for the study of genetically modified mice. *Behav Brain Res*. 2001;124(1):33–46.
82. Deacon RMJ. Measuring the Strength of Mice. *J Vis Exp*. 2013;(76):2610.
83. Sishi B, Loos B, Ellis B, Smith W, du Toit EF, Engelbrecht A-M. Diet-induced obesity alters signalling pathways and induces atrophy and apoptosis in skeletal muscle in a prediabetic rat model: Diet-induced obesity and skeletal muscle. *Exp Physiol*. 2011;96(2):179–93.
84. Alquier T, Poitout V. Considerations and guidelines for mouse metabolic phenotyping in diabetes research. *Diabetologia*. 2018;61(3):526–38.

85. Heydemann A. An Overview of Murine High Fat Diet as a Model for Type 2 Diabetes Mellitus. *J Diabetes Res*. 2016;2016:1–14.
86. Hales CM, Fryar CD, Carroll MD, Freedman DS, Ogden CL. Trends in Obesity and Severe Obesity Prevalence in US Youth and Adults by Sex and Age, 2007-2008 to 2015-2016. *JAMA*. 2018;319(16):1723–5.
87. NCD Risk Factor Collaboration (NCD-RisC). Trends in adult body-mass index in 200 countries from 1975 to 2014: a pooled analysis of 1698 population-based measurement studies with 19·2 million participants. *Lancet Lond Engl*. 2016;387(10026):1377–96.
88. Gregor MF, Hotamisligil GS. Inflammatory mechanisms in obesity. *Annu Rev Immunol*. 2011;29:415–45.
89. Kusminski CM, Shetty S, Orci L, Unger RH, Scherer PE. Diabetes and apoptosis: lipotoxicity. *Apoptosis*. 2009;14(12):1484–95.
90. Manna P, Jain SK. Obesity, Oxidative Stress, Adipose Tissue Dysfunction, and the Associated Health Risks: Causes and Therapeutic Strategies. *Metab Syndr Relat Disord*. 2015;13(10):423–44.
91. Reilly SM, Saltiel AR. Adapting to obesity with adipose tissue inflammation. *Nat Rev Endocrinol*. 2017;13(11):633–43.
92. Campbell TL, Mitchell AS, McMillan EM, et al. High-fat feeding does not induce an autophagic or apoptotic phenotype in female rat skeletal muscle. *Exp Biol Med Maywood NJ*. 2015;240(5):657–68.
93. Biswas SK. Does the Interdependence between Oxidative Stress and Inflammation Explain the Antioxidant Paradox? *Oxid Med Cell Longev*. 2016;2016:1–9.
94. Marseglia L, Manti S, D'Angelo G, et al. Oxidative Stress in Obesity: A Critical Component in Human Diseases. *Int J Mol Sci*. 2014;16(1):378–400.
95. McMurray F, Patten DA, Harper M-E. Reactive Oxygen Species and Oxidative Stress in Obesity-Recent Findings and Empirical Approaches: ROS and Oxidative Stress in Obesity. *Obesity*. 2016;24(11):2301–10.
96. Snel M, Jonker JT, Schoones J, et al. Ectopic fat and insulin resistance: pathophysiology and effect of diet and lifestyle interventions. *Int J Endocrinol*. 2012;2012:983814.
97. Matsuda M, Shimomura I. Increased oxidative stress in obesity: Implications for metabolic syndrome, diabetes, hypertension, dyslipidemia, atherosclerosis, and cancer. *Obes Res Clin Pract*. 2013;7(5):e330–41.
98. Huang C-J, McAllister MJ, Slusher AL, Webb HE, Mock JT, Acevedo EO. Obesity-Related Oxidative Stress: the Impact of Physical Activity and Diet Manipulation. *Sports Med - Open*. 2015;1(1):32.

99. Dłudla P, Nkambule B, Jack B, et al. Inflammation and Oxidative Stress in an Obese State and the Protective Effects of Gallic Acid. *Nutrients*. 2018;11(1):23.
100. Furukawa S, Fujita T, Shimabukuro M, et al. Increased oxidative stress in obesity and its impact on metabolic syndrome. *J Clin Invest*. 2004;114(12):1752–61.
101. Issa N, Lachance G, Bellmann K, Laplante M, Stadler K, Marette A. Cytokines promote lipolysis in 3T3-L1 adipocytes through induction of NADPH oxidase 3 expression and superoxide production. *J Lipid Res*. 2018;59(12):2321–8.
102. Murdolo G, Piroddi M, Luchetti F, et al. Oxidative stress and lipid peroxidation by-products at the crossroad between adipose organ dysregulation and obesity-linked insulin resistance. *Biochimie*. 2013;95(3):585–94.
103. Meex RCR, Blaak EE, Loon LJC. Lipotoxicity plays a key role in the development of both insulin resistance and muscle atrophy in patients with type 2 diabetes. *Obes Rev*. 2019;20(9):1205–17.
104. Inoguchi T, Li P, Umeda F, et al. High glucose level and free fatty acid stimulate reactive oxygen species production through protein kinase C--dependent activation of NAD(P)H oxidase in cultured vascular cells. *Diabetes*. 2000;49(11):1939–45.
105. Weisberg SP, McCann D, Desai M, Rosenbaum M, Leibel RL, Ferrante AW. Obesity is associated with macrophage accumulation in adipose tissue. *J Clin Invest*. 2003;112(12):1796–808.
106. Xu H, Barnes GT, Yang Q, et al. Chronic inflammation in fat plays a crucial role in the development of obesity-related insulin resistance. *J Clin Invest*. 2003;112(12):1821–30.
107. Lackey DE, Olefsky JM. Regulation of metabolism by the innate immune system. *Nat Rev Endocrinol*. 2016;12(1):15–28.
108. Grimm S, Ott C, Hörlacher M, Weber D, Höhn A, Grune T. Advanced-glycation-end-product-induced formation of immunoproteasomes: involvement of RAGE and Jak2/STAT1. *Biochem J*. 2012;448(1):127–39.
109. Kästle M, Reeg S, Rogowska-Wrzesinska A, Grune T. Chaperones, but not oxidized proteins, are ubiquitinated after oxidative stress. *Free Radic Biol Med*. 2012;53(7):1468–77.
110. Salvestrini V, Sell C, Lorenzini A. Obesity May Accelerate the Aging Process. *Front Endocrinol*. 2019;10:266.
111. Fernando R, Drescher C, Nowotny K, Grune T, Castro JP. Impaired proteostasis during skeletal muscle aging. *Free Radic Biol Med*. 2019;132:58–66.
112. Goodpaster BH, Chomentowski P, Ward BK, et al. Effects of physical activity on strength and skeletal muscle fat infiltration in older adults: a randomized controlled trial. *J Appl Physiol*. 2008;105(5):1498–503.

113. Marcus RL, Addison O, Kidde JP, Dibble LE, Lastayo PC. Skeletal muscle fat infiltration: Impact of age, inactivity, and exercise. *J Nutr Health Aging*. 2010;14(5):362–6.
114. Lecker SH, Goldberg AL, Mitch WE. Protein Degradation by the Ubiquitin–Proteasome Pathway in Normal and Disease States. *J Am Soc Nephrol*. 2006;17(7):1807–19.
115. Morimoto RI, Cuervo AM. Proteostasis and the Aging Proteome in Health and Disease. *J Gerontol A Biol Sci Med Sci*. 2014;69(Suppl 1):S33–8.
116. Shang F, Taylor A. Ubiquitin–proteasome pathway and cellular responses to oxidative stress. *Free Radic Biol Med*. 2011;51(1):5–16.
117. Turpin SM, Ryall JG, Southgate R, et al. Examination of ‘lipotoxicity’ in skeletal muscle of high-fat fed and *ob / ob* mice: Skeletal muscle lipotoxicity *in vivo*. *J Physiol*. 2009;587(7):1593–605.
118. Zhou Q, Du J, Hu Z, Walsh K, Wang XH. Evidence for Adipose-Muscle Cross Talk: Opposing Regulation of Muscle Proteolysis by Adiponectin and Fatty Acids. *Endocrinology*. 2007;148(12):5696–705.
119. Grune T, Catalgol B, Licht A, et al. HSP70 mediates dissociation and reassociation of the 26S proteasome during adaptation to oxidative stress. *Free Radic Biol Med*. 2011;51(7):1355–64.
120. Baumann CW, Kwak D, Ferrington DA, Thompson LV. Downhill exercise alters immunoproteasome content in mouse skeletal muscle. *Cell Stress Chaperones*. 2018;23(4):507–17.
121. Johnsen A, France J, Sy MS, Harding CV. Down-regulation of the transporter for antigen presentation, proteasome subunits, and class I major histocompatibility complex in tumor cell lines. *Cancer Res*. 1998;58(16):3660–7.
122. Li F, Nie H, Tian C, et al. Ablation and Inhibition of the Immunoproteasome Catalytic Subunit LMP7 Attenuate Experimental Abdominal Aortic Aneurysm Formation in Mice. *J Immunol Baltim Md 1950*. 2019;202(4):1176–85.
123. Muchamuel T, Basler M, Aujay MA, et al. A selective inhibitor of the immunoproteasome subunit LMP7 blocks cytokine production and attenuates progression of experimental arthritis. *Nat Med*. 2009;15(7):781–7.
124. Rouette A, Trofimov A, Haberl D, et al. Expression of immunoproteasome genes is regulated by cell-intrinsic and –extrinsic factors in human cancers. *Sci Rep*. 2016;6(1):1–14.
125. Lee HS, Suh JY, Kang B-C, Lee E. Lipotoxicity dysregulates the immunoproteasome in podocytes and kidneys in type 2 diabetes. *Am J Physiol-Ren Physiol*. 2021;320(4):F548–58.
126. Varshavsky A. The early history of the ubiquitin field. *Protein Sci*. 2006;15(3):647–54.

127. Wolf DH, Hilt W. The proteasome: a proteolytic nanomachine of cell regulation and waste disposal. *Biochim Biophys Acta BBA - Mol Cell Res.* 2004;1695(1–3):19–31.
128. Kors S, Geijtenbeek K, Reits E, Schipper-Krom S. Regulation of Proteasome Activity by (Post-)transcriptional Mechanisms. *Front Mol Biosci.* 2019;6:48.
129. Ferrington DA, Husom AD, Thompson LV. Altered proteasome structure, function, and oxidation in aged muscle. *FASEB J Off Publ Fed Am Soc Exp Biol.* 2005;19(6):644–6.
130. Chen C-NJ, Graber TG, Bratten WM, Ferrington DA, Thompson LV. Immunoproteasome in animal models of Duchenne muscular dystrophy. *J Muscle Res Cell Motil.* 2014;35(2):191–201.
131. Bhattarai S, Ghannam K, Krause S, et al. The immunoproteasomes are key to regulate myokines and MHC class I expression in idiopathic inflammatory myopathies. *J Autoimmun.* 2016;75:118–29.
132. Gan J, Leestemaker Y, Sapmaz A, Ovaa H. Highlighting the Proteasome: Using Fluorescence to Visualize Proteasome Activity and Distribution. *Front Mol Biosci.* 2019;6:14.
133. Thibaudeau TA, Smith DM. A Practical Review of Proteasome Pharmacology. *Pharmacol Rev.* 2019;71(2):170–97.
134. Kisselev AF, van der Linden WA, Overkleeft HS. Proteasome Inhibitors: An Expanding Army Attacking a Unique Target. *Chem Biol.* 2012;19(1):99–115.
135. Moravec RA, O’Brien MA, Daily WJ, Scurria MA, Bernad L, Riss TL. Cell-based bioluminescent assays for all three proteasome activities in a homogeneous format. *Anal Biochem.* 2009;387(2):294–302.
136. Crawford LJA, Walker B, Ovaa H, et al. Comparative Selectivity and Specificity of the Proteasome Inhibitors BzLLLCOCHO, PS-341, and MG-132. *Cancer Res.* 2006;66(12):6379–86.
137. Basler M, Lindstrom MM, LaStant JJ, et al. Co-inhibition of immunoproteasome subunits LMP2 and LMP7 is required to block autoimmunity. *EMBO Rep* [Internet]. 2018 [cited 2020 May 3];19(12) Available from: <https://onlinelibrary.wiley.com/doi/abs/10.15252/embr.201846512>. doi:10.15252/embr.201846512.
138. Blackburn C, Gigstad KM, Hales P, et al. Characterization of a new series of non-covalent proteasome inhibitors with exquisite potency and selectivity for the 20S β 5-subunit. *Biochem J.* 2010;430(3):461–76.
139. Husom AD, Peters EA, Kolling EA, Fugere NA, Thompson LV, Ferrington DA. Altered proteasome function and subunit composition in aged muscle. *Arch Biochem Biophys.* 2004;421(1):67–76.

140. Strucksberg K-H, Tangavelou K, Schröder R, Clemen CS. Proteasomal activity in skeletal muscle: A matter of assay design, muscle type, and age. *Anal Biochem.* 2010;399(2):225–9.
141. Yang M, Ding X, Luo L, Hao Q, Dong B. Disability Associated With Obesity, Dynapenia and Dynapenic-Obesity in Chinese Older Adults. *J Am Med Dir Assoc.* 2014;15(2):150.e11-150.e16.
142. Alexandre T da S, Scholes S, Ferreira Santos JL, Duarte YA de O, de Oliveira C. The combination of dynapenia and abdominal obesity as a risk factor for worse trajectories of IADL disability among older adults. *Clin Nutr Edinb Scotl.* 2018;37(6 Pt A):2045–53.
143. Alexandre T da S, Scholes S, Santos JLF, de Oliveira C. Dynapenic Abdominal Obesity as a Risk Factor for Worse Trajectories of ADL Disability Among Older Adults: The ELSA Cohort Study. *J Gerontol Ser A.* 2019;74(7):1112–8.
144. National Research Council (US) Subcommittee on Laboratory Animal Nutrition. *Nutrient Requirements of the Mouse.* National Academies Press (US); 1995. [cited 2019 May 26] Available from: <https://www.ncbi.nlm.nih.gov/books/NBK231918/>.
145. Ayala JE, Samuel VT, Morton GJ, et al. Standard operating procedures for describing and performing metabolic tests of glucose homeostasis in mice. *Dis Model Mech.* 2010;3(9–10):525–34.
146. Chusyd DE, Wang D, Huffman DM, Nagy TR. Relationships between Rodent White Adipose Fat Pads and Human White Adipose Fat Depots. *Front Nutr.* 2016;3:10.
147. Pickering AM, Davies KJA. Degradation of Damaged Proteins. *Progress in Molecular Biology and Translational Science.* Elsevier; 2012. p. 227–48. [cited 2020 Apr 16] Available from: <https://linkinghub.elsevier.com/retrieve/pii/B9780123978639000067>.
148. Jensen C, Teng Y. Is It Time to Start Transitioning From 2D to 3D Cell Culture? *Front Mol Biosci.* 2020;7:33.
149. Okada K, Wangpoengtrakul C, Osawa T, Toyokuni S, Tanaka K, Uchida K. 4-Hydroxy-2-nonenal-mediated impairment of intracellular proteolysis during oxidative stress. Identification of proteasomes as target molecules. *J Biol Chem.* 1999;274(34):23787–93.
150. DeFronzo RA, Tripathy D. Skeletal muscle insulin resistance is the primary defect in type 2 diabetes. *Diabetes Care.* 2009;32 Suppl 2:S157-163.
151. Kisselev AF, Akopian TN, Castillo V, Goldberg AL. Proteasome Active Sites Allosterically Regulate Each Other, Suggesting a Cyclical Bite-Chew Mechanism for Protein Breakdown. *Mol Cell.* 1999;4(3):395–402.
152. Jang YC, Sinha M, Cerletti M, Dall’Osso C, Wagers AJ. Skeletal muscle stem cells: effects of aging and metabolism on muscle regenerative function. *Cold Spring Harb Symp Quant Biol.* 2011;76:101–11.

153. Landers KA, Hunter GR, Wetzstein CJ, Bamman MM, Weinsier RL. The interrelationship among muscle mass, strength, and the ability to perform physical tasks of daily living in younger and older women. *J Gerontol A Biol Sci Med Sci*. 2001;56(10):B443-448.
154. Julian V, Thivel D, Costes F, et al. Eccentric Training Improves Body Composition by Inducing Mechanical and Metabolic Adaptations: A Promising Approach for Overweight and Obese Individuals. *Front Physiol*. 2018;9:1013.
155. Julian V, Thivel D, Miguet M, et al. Eccentric cycling is more efficient in reducing fat mass than concentric cycling in adolescents with obesity. *Scand J Med Sci Sports*. 2019;29(1):4–15.
156. Minetti AE, Moia C, Roi GS, Susta D, Ferretti G. Energy cost of walking and running at extreme uphill and downhill slopes. *J Appl Physiol*. 2002;93(3):1039–46.
157. Xie X, Bi H-L, Lai S, et al. The immunoproteasome catalytic $\beta 5i$ subunit regulates cardiac hypertrophy by targeting the autophagy protein ATG5 for degradation. *Sci Adv*. 2019;5(5):eaau0495.
158. Akhmedov D, Berdeaux R. The effects of obesity on skeletal muscle regeneration. *Front Physiol* [Internet]. 2013 [cited 2020 Apr 16];4 Available from: <http://journal.frontiersin.org/article/10.3389/fphys.2013.00371/abstract>. doi:10.3389/fphys.2013.00371.
159. Allen DG, Lamb GD, Westerblad H. Skeletal Muscle Fatigue: Cellular Mechanisms. *Physiol Rev*. 2008;88(1):287–332.